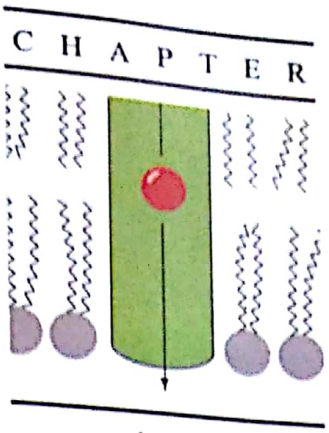


18

Transport through Membranes

1. **Thermodynamics of Transport**
2. **Kinetics and Mechanisms of Transport**
 A. Nonmediated Transport
 B. Kinetics of Mediated Transport: Glucose Transport into Erythrocytes
 C. Ionophores and Porins
 D. Mechanism of Passive-Mediated Glucose Transport
3. **ATP-Driven Active Transport**
 A. (Na^+-K^+)-ATPase of Plasma Membranes
 B. Ca^{2+}-ATPase
 C. (H^+-K^+)-ATPase of Gastric Mucosa
 D. Group Translocation
4. **Ion Gradient-Driven Active Transport**
 A. Na^+-Glucose Symport
 B. Lactose Permease
 C. ADP-ATP Translocator

Metabolism occurs within cells that are separated from their environments by plasma membranes. Eukaryotic cells, in addition, are compartmentalized by intracellular membranes that form the boundaries and internal structures of their various organelles. The nonpolar cores of biological membranes make them highly impermeable to most ionic and polar substances so that *these substances can traverse membranes only through the action of specific* ***transport proteins.*** Such proteins are therefore required to mediate all transmembrane movements of ions, such as Na^+, K^+, Ca^{2+}, and Cl^-, as well as metabolites such as pyruvate, amino acids, sugars, and nucleotides. Transport proteins are also responsible for all biological electrochemical phenomena. In this chapter, we discuss the thermodynamics, kinetics, and chemical mechanisms of these membrane transport systems.

1. THERMODYNAMICS OF TRANSPORT

As we saw in Section 3-4A, the free energy of a solute, A, varies with its concentration:

$$\overline{G}_A - \overline{G}_A^{\circ\prime} = RT \ln [A] \qquad [18.1]$$

where $\overline{G}_A$ is the **chemical potential** (partial molar free energy) of A (the bar indicates quantity per mole) and $\overline{G}_A^{\circ\prime}$ is the chemical potential of its standard state. Strictly speaking, this equation applies only to ideal solutions; for nonideal (real) solutions, molar concentrations must be replaced by activities (Appendix to Chapter 3). This added complication is unnecessary for our purposes, however, because at the low physiological concentrations of biological substances, activities closely approach their corresponding molar concentrations in value.

The diffusion of a substance between two sides of a membrane

$$A(out) \rightleftharpoons A(in)$$

thermodynamically resembles a chemical equilibration. A difference in the concentrations of the substance on two

sides of a membrane generates a chemical potential difference:

$$\Delta\overline{G}_A = \overline{G}_A(in) - \overline{G}_A(out) = RT \ln\left(\frac{[A]_{in}}{[A]_{out}}\right) \quad [18.2]$$

Consequently, if the concentration of A outside the membrane is greater than that inside, $\Delta\overline{G}_A$ for the transfer of A from outside to inside will be negative and the spontaneous net flow of A will be inward. If, however, [A] is greater inside than outside, $\Delta\overline{G}_A$ is positive and an inward net flow of A can only occur if an exergonic process, such as ATP hydrolysis, is coupled to it to make the overall free energy change negative.

Membrane Potentials Arise from Transmembrane Concentration Differences of Ionic Substances

The permeabilities of biological membranes to ions such as H^+, Na^+, K^+, Cl^-, and Ca^{2+} are controlled by specific membrane-embedded transport systems that we shall discuss in later sections. *The resulting charge differences across a biological membrane generate an electric potential difference,* $\Delta\Psi = \Psi(in) - \Psi(out)$, where $\Delta\Psi$ is termed the **membrane potential.** Consequently, if A is ionic, Eq. [18.2] must be amended to include the electrical work required to transfer a mole of A across the membrane from outside to inside:

$$\Delta\overline{G}_A = RT \ln\left(\frac{[A]_{in}}{[A]_{out}}\right) + Z_A\mathcal{F}\,\Delta\Psi \quad [18.3]$$

where Z_A is the ionic charge of A; $\mathcal{F}$, the Faraday constant, is the charge on a mole of electrons (96,494 $C \cdot mol^{-1}$); and, $\overline{G}_A$ is now termed the **electrochemical potential** of A.

Membrane potentials in living cells can be measured directly with microelectrodes. $\Delta\Psi$ values of −100 mV (inside negative) are not uncommon (note that 1 V = 1 $J \cdot C^{-1}$). Thus the last term of Eq. [18.3] is often significant for ionic substances.

2. KINETICS AND MECHANISMS OF TRANSPORT

Thermodynamics indicates whether a given transport process will be spontaneous but, as we saw for chemical and enzymatic reactions, provides no indication of the rates of these processes. Kinetic analyses of transport processes together with mechanistic studies have nevertheless permitted these processes to be characterized. There are two types of transport processes: **Nonmediated transport** and **mediated transport.** Nonmediated transport occurs through simple diffusion. In contrast, *mediated transport occurs through the action of specific carrier proteins* that are variously called **carriers, permeases, porters, translocases, translocators,** and **transporters.** Mediated transport is further classified into two categories depending on the thermodynamics of the system:

1. **Passive-mediated transport** or **facilitated diffusion** in which specific molecules flow from high concentration to low concentration so as to equilibrate their concentration gradients.
2. **Active transport** in which specific molecules are transported from low concentration to high concentration, that is, against their concentration gradients. Such an endergonic process must be coupled to a sufficiently exergonic process to make it favorable.

In this section, we consider the nature of nonmediated transport and then compare it to passive-mediated transport as exemplified by the erythrocyte glucose transporter, ionophores, and porins. Active transport is examined in succeeding sections.

A. Nonmediated Transport

The driving force for the nonmediated flow of a substance A through a medium is A's electrochemical potential gradient. This relationship is expressed by the **Nernst–Planck equation:**

$$J_A = -[A]U_A\,(d\overline{G}_A/dx) \quad [18.4]$$

where J_A is the flux (rate of passage per unit area) of A, x is distance, $d\overline{G}_A/dx$ is the electrochemical potential gradient of A, and U_A is its **mobility** (velocity per unit force) in the medium. If we assume, for simplicity, that A is an uncharged molecule so that $\overline{G}_A$ is given by Eq. [18.1], the Nernst–Planck equation reduces to

$$J_A = -D_A\,(d[A]/dx) \quad [18.5]$$

where $D_A \equiv RTU_A$ is the **diffusion coefficient** of A in the medium of interest. This is **Fick's first law of diffusion,** which states that *a substance diffuses in the direction that eliminates its concentration gradient,* $d[A]/dx$, *at a rate proportional to the magnitude of this gradient.*

For a membrane of thickness x, Eq. [18.5] is approximated by

$$J_A = \frac{D_A}{x}([A]_{out} - [A]_{in}) = P_A([A]_{out} - [A]_{in}) \quad [18.6]$$

where D_A is the diffusion coefficient of A inside the membrane and $P_A = D_A/x$ is termed the membrane's **permeability coefficient** for A. The permeability coefficient is indicative of the solute's tendency to transfer from the aqueous solvent to the membrane's nonpolar core. It should therefore vary with the ratio of the solute's solubility in a nonpolar solvent resembling the membrane's core (e.g., olive oil) to that in water, a quantity known as the solute's **partition coefficient** between the two solvents. Indeed, the fluxes of

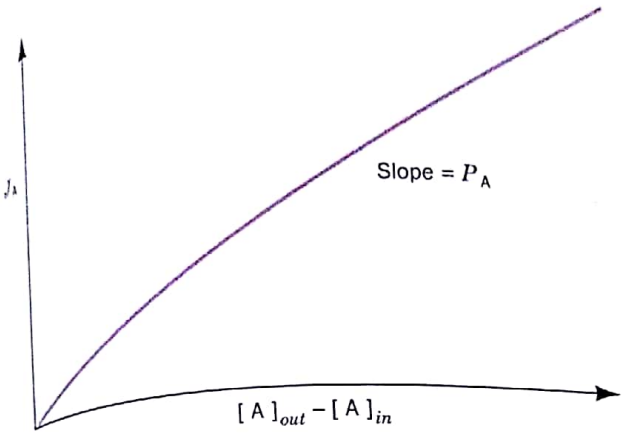


FIGURE 18-1. The linear relationship between diffusional flux (J_A) and $([A]_{out} - [A]_{in})$ across a semipermeable membrane; see Eq. [18.6].

many nonelectrolytes across erythrocyte membranes vary linearly with their concentration differences across the membrane as predicted by Eq. [18.6] (Fig. 18-1). Moreover, their permeability coefficients, as obtained from the slopes of plots such as Fig. 18-1, correlate rather well with their measured partition coefficients between nonpolar solvents and water (Fig. 18-2).

B. Kinetics of Mediated Transport: Glucose Transport into Erythrocytes

Despite the success of the foregoing model in predicting the rates at which many molecules pass through membranes, there are numerous combinations of solutes and membranes that do not obey Eq. [18.6]. The flux in such a system is not linear with the solute concentration difference

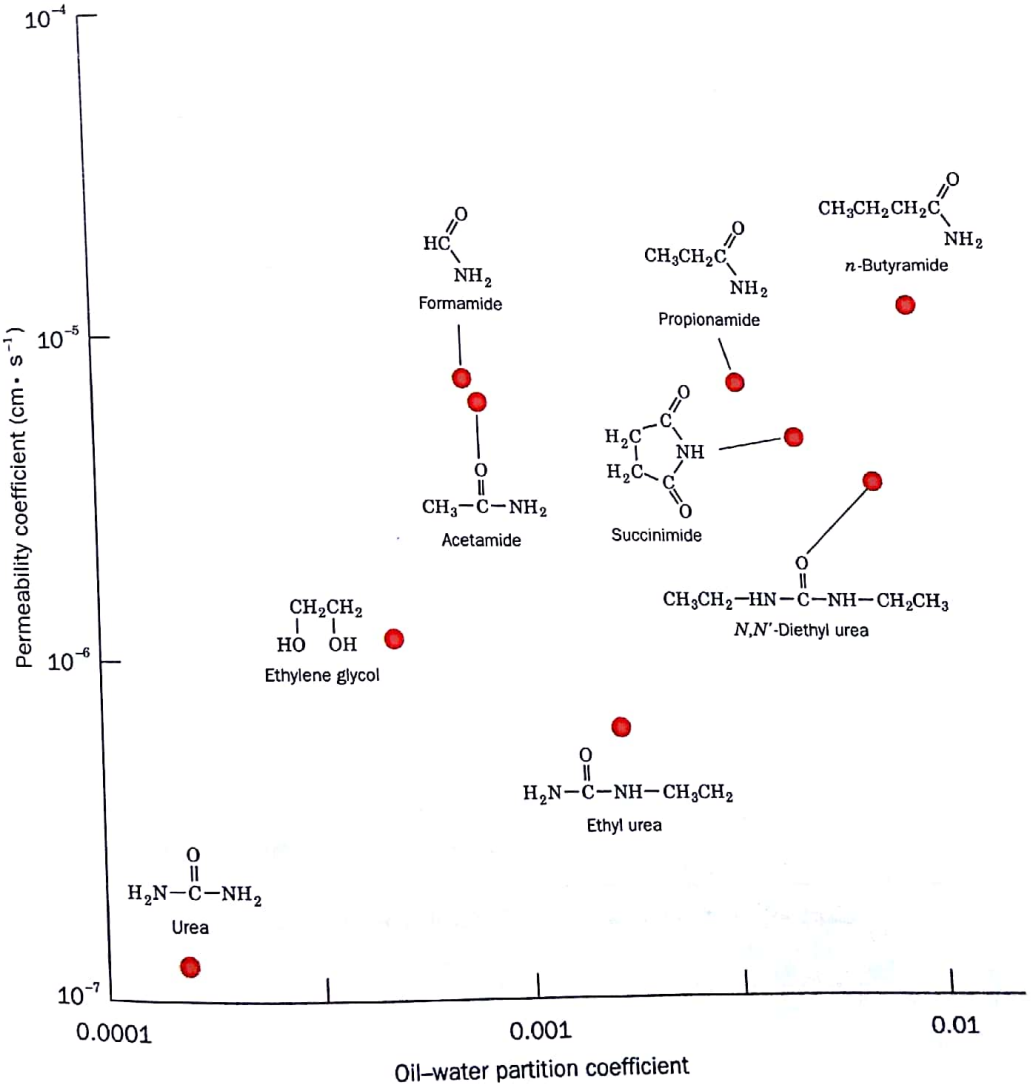


FIGURE 18-2. The permeability coefficients of various organic molecules in plasma membranes from the alga *Nitella mucronata* versus their partition coefficients between olive oil and water (a measure of a molecule's polarity). This more or less linear log–log plot indicates that the rate-limiting step for the nonmediated entry of a molecule into a cell is its passage through the membrane's hydrophobic core. [Based on data from Collander, R., *Physiol. Plant.* **7**, 433–434 (1954).]

across the corresponding membrane (Fig. 18-3) and, furthermore, the solute's permeability coefficient is much larger than is expected on the basis of its partition coefficient. Such behavior indicates that *these solutes are conveyed across membranes in complex with carrier molecules; that is, they undergo mediated transport.*

The system that transports glucose across the erythrocyte membrane provides a well-characterized example of passive-mediated transport: It invariably transports glucose down its concentration gradient but not at the rate predicted by Eq. [18.6]. Indeed, the **erythrocyte glucose transporter** exhibits four characteristics that differentiate mediated from nonmediated transport: (1) *speed and specificity,* (2) *saturation kinetics,* (3) *susceptibility to competitive inhibition, and* (4) *susceptibility to chemical inactivation.* In the following paragraphs we shall see how the erythrocyte glucose transporter exhibits these qualities.

Speed and Specificity

Table 18-1 indicates that the permeability coefficients of D-glucose and D-mannitol in synthetic bilayers, and that of D-mannitol in the erythrocyte membrane, are in reasonable agreement with the values calculated from the diffusion and partition coefficients of these sugars in olive oil. However, the experimentally determined permeability coefficient for D-glucose in the erythrocyte membrane is four orders of magnitude greater than its predicted value. *The erythrocyte membrane must therefore contain a system that rapidly transports glucose and that can distinguish D-glucose from D-mannitol.*

Saturation Kinetics

The concentration dependence of glucose transport indicates that its flux obeys the relationship:

$$J_A = \frac{J_{max}[A]}{K_M + [A]} \qquad [18.7]$$

This **saturation function** has a familiar hyperbolic form (Fig. 18-3). We have seen it in the equation describing the binding of O_2 to myoglobin (Eq. [9.2]) and in the Michaelis–Menten equation describing the rates of enzymatic reactions (Eq. [13.24]). Here, as before, K_M may be defined operationally as the concentration of glucose when the transport flux is half of its maximal rate, $J_{max}/2$. *This observation of* ***saturation kinetics*** *for glucose transport was the first evidence that a specific saturable number of sites on the membrane were involved in the transport of any substance.*

TABLE 18-1. PERMEABILITY COEFFICIENTS OF NATURAL AND SYNTHETIC MEMBRANES TO D-GLUCOSE AND D-MANNITOL AT 25°C

Membrane Preparation	Permeability Coefficient ($cm \cdot s^{-1}$)	
	D-Glucose	D-Mannitol
Synthetic lipid bilayer	2.4×10^{-10}	4.4×10^{-11}
Calculated nonmediated diffusion	4×10^{-9}	3×10^{-9}
Intact human erythrocyte	2.0×10^{-4}	5×10^{-9}

Source: Jung, C.Y., *in* Surgenor, D. (Ed.), *The Red Blood Cell,* Vol. 2, p. 709, Academic Press (1975).

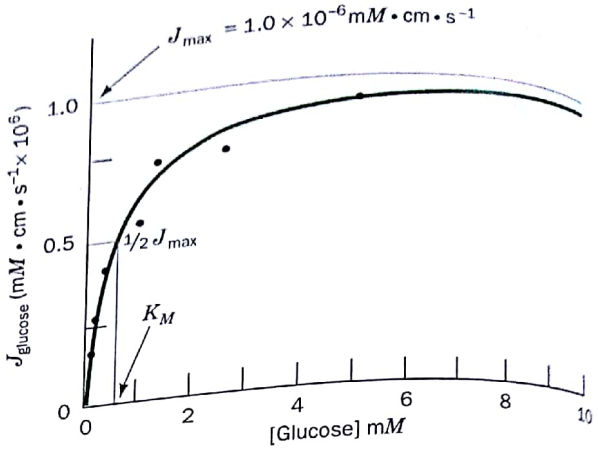


FIGURE 18-3. The variation of glucose flux into human erythrocytes with the external glucose concentration at 5°C. The black dots are experimentally determined data points, and the solid green line is computed from Eq. [18.7] with $J_{max} = 1.0 \times 10^{-6}$ $mM \cdot cm \cdot s^{-1}$ and $K_M = 0.5$ mM. The nonmediated glucose flux increases linearly with [glucose] (Fig. 18-1) but would not visibly depart from the baseline on the scale of this drawing. [Based on data from Stein, W.D., *Movement of Molecules across Membranes, p.* 134, Academic Press (1967).]

The transport process can be described by a simple four-step kinetic scheme involving binding, transport, dissociation, and recovery (Fig. 18-4). Its binding and dissociation steps are analogous to the recognition of a substrate and the release of product by an enzyme. The mechanisms of transport and recovery are under active investigation and are discussed in Section 18-2D.

Susceptibility to Competitive Inhibition

Many compounds structurally similar to D-glucose inhibit glucose transport. A double-reciprocal plot (Section 13-2B) for the flux of glucose into erythrocytes in the presence or absence of 6-*O*-benzyl-D-galactose (Fig. 18-5) shows behavior typical of competitive inhibition of glucose transport (competitive inhibition of enzymes is discussed in Section 13-3A). *Susceptibility to competitive inhibition indicates that there is a limited number of sites available for mediated transport.*

Susceptibility to Chemical Inactivation

Treatment of erythrocytes with $HgCl_2$, which reacts with protein sulfhydryl groups (Section 6-2) and thus inactivates many enzymes, causes the rapid, saturatable flux of glucose to disappear so that its permeability constant approaches that of mannitol. *The erythrocyte glucose transport sys-*

gen's susceptibility to such protein-modifying agents indicates that it, in fact, is a protein.

All of the above observations indicate that *glucose transport across the erythrocyte membrane is mediated by a limited number of protein carriers.* Before we discuss the mechanism of this transport system, however, we shall examine some simpler models of facilitated diffusion.

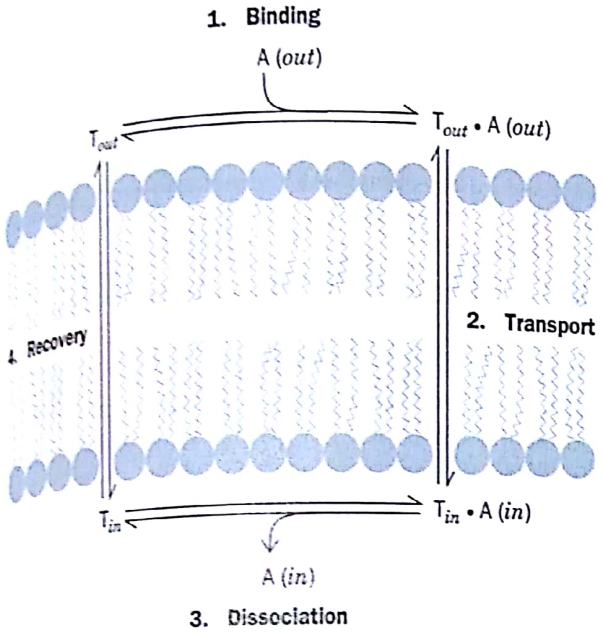


FIGURE 18-4. A general kinetic scheme for membrane transport involving four steps: binding, transport, dissociation, and recovery. T is the transport protein whose binding site for solute A is located on either the inner or the outer side of the membrane at any one time.

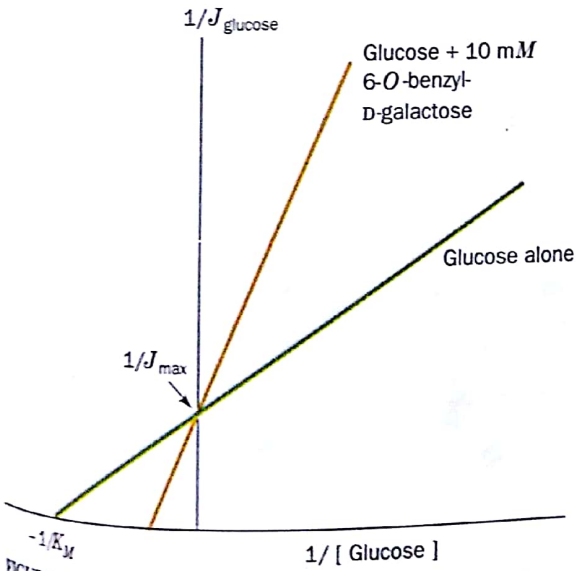


FIGURE 18-5. Double-reciprocal plots for the net flux of glucose into erythrocytes in the presence and absence of 6-*O*-benzyl-D-galactose. The pattern is that of competitive inhibition. [After Barnett, J.E.G., Holman, G.D., Chalkley, R.A., and Munday, K.A., *Biochem. J.* **145**, 422 (1975).]

C. Ionophores and Porins

Our understanding of mediated transport has been enhanced by the study of **ionophores,** substances that vastly increase the permeability of membranes to particular ions.

Ionophores May Be Carriers or Channel Formers

Ionophores are organic molecules of diverse types, many of which are antibiotics of bacterial origin. Cells and organelles actively maintain concentration gradients of various ions across their membranes (Section 18-3A). The antibiotic properties of ionophores arise from their tendency to discharge these vital concentration gradients.

There are two types of ionophores:

1. ***Carriers,*** *which increase the permeabilities of membranes to their selected ion by binding it, diffusing through the membrane, and releasing the ion on the other side (Fig. 18-6a).* For net transport to occur, the uncomplexed ionophore must then return to the original side of the membrane ready to repeat the process. Carriers therefore share the common property that *their ionic complexes are soluble in nonpolar solvents.*
2. ***Channel formers,*** *which form transmembrane channels or pores through which their selected ions can diffuse (Fig. 18-6b).*

Both types of ionophores transport ions at a remarkable rate. For example, a single molecule of the carrier antibiotic **valinomycin** transports up to 10^4 K^+ ions/s across a membrane. Channel formers have an even greater ion throughput; for example, each membrane channel composed of the antibiotic **gramicidin A** permits the passage of over 10^7 K^+ ions/s. Clearly, the presence of either type of ionophore, even in small amounts, greatly increases the permeability of a membrane towards the specific ions transported. However, *since ionophores passively permit ions to diffuse across*

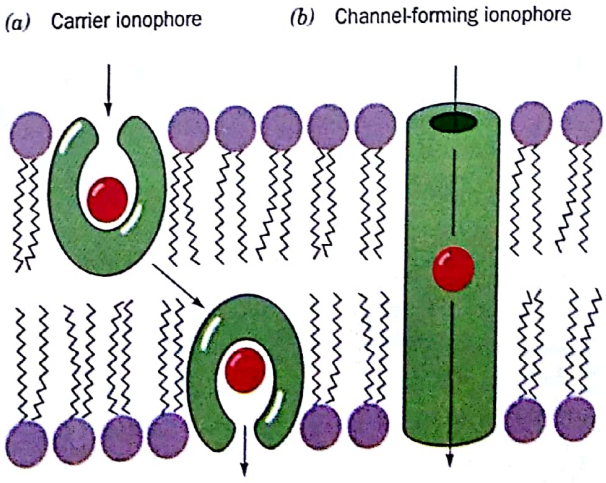
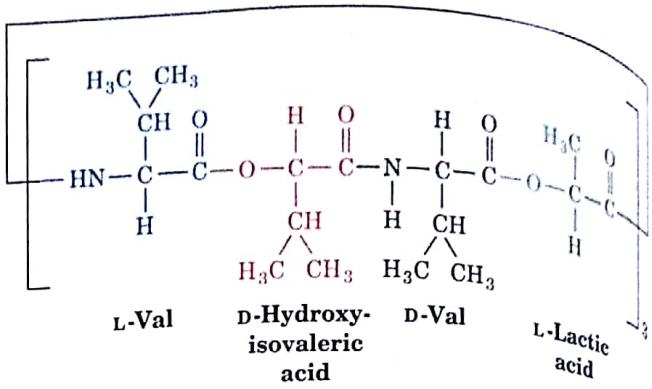


FIGURE 18-6. The ion transport modes of ionophores: (*a*) Carrier ionophores transport ions by diffusing through the lipid bilayer. (*b*) Channel-forming ionophores span the membrane with a channel through which ions can diffuse.

a membrane in either direction, their effect can only be to equilibrate the concentrations of their selected ions across the membrane.

Carriers and channel formers are easily distinguished experimentally through differences in the temperature dependence of their action. Carriers depend on their ability to diffuse freely across the membrane. Consequently, cooling a membrane below its transition temperature (the temperature below which it becomes a gel-like solid; Section 11-2B) essentially eliminates its ionic permeability in the presence of carriers. In contrast, membrane permeability in the presence of channel formers is rather insensitive to temperature because, once in place, channel formers need not move to mediate ion transport.



Valinomycin

FIGURE 18-7. Valinomycin is a cyclic depsipeptide (has both ester and amide bonds) that contains both D- and L-amino acids.

The K^+–Valinomycin Complex Has a Polar Interior and a Hydrophobic Exterior

Valinomycin, which is perhaps the best characterized carrier ionophore, specifically binds K^+ and the biologically unimportant Rb^+. It is a **cyclic depsipeptide** that has both D- and L-amino acid residues (Fig. 18-7; a depsipeptide contains ester linkages as well as peptide bonds). The X-ray structure of valinomycin's K^+ complex (Fig. 18-8*a*) indicates that the K^+ is octahedrally coordinated by the carbonyl groups of its 6 Val residues, which also form its ester linkages. The cyclic, intramolecularly hydrogen bonded valinomycin backbone follows a zigzag path that surrounds the K^+ coordination shell with a sinuous molecular bracelet. *Its methyl and isopropyl side chains project outward from the bracelet to provide the spheroidal complex with a hydrophobic exterior that makes it soluble in nonpolar solvents and in the hydrophobic cores of lipid bilayers.* Uncomplexed valinomycin (Fig. 18-8*b*) has a more open conformation than its K^+ complex, which presumably facilitates the rapid binding of K^+.

K^+ (ionic radius, $r = 1.33$ Å) and Rb^+ ($r = 1.49$ Å) fit snugly into valinomycin's coordination site. However, the rigidity of the valinomycin complex makes this site too large to accommodate Na^+ ($r = 0.95$ Å) or Li^+ ($r = 0.60$ Å) properly; that is, valinomycin's six carbonyl oxygen atoms cannot simultaneously coordinate these ions. Complexes of

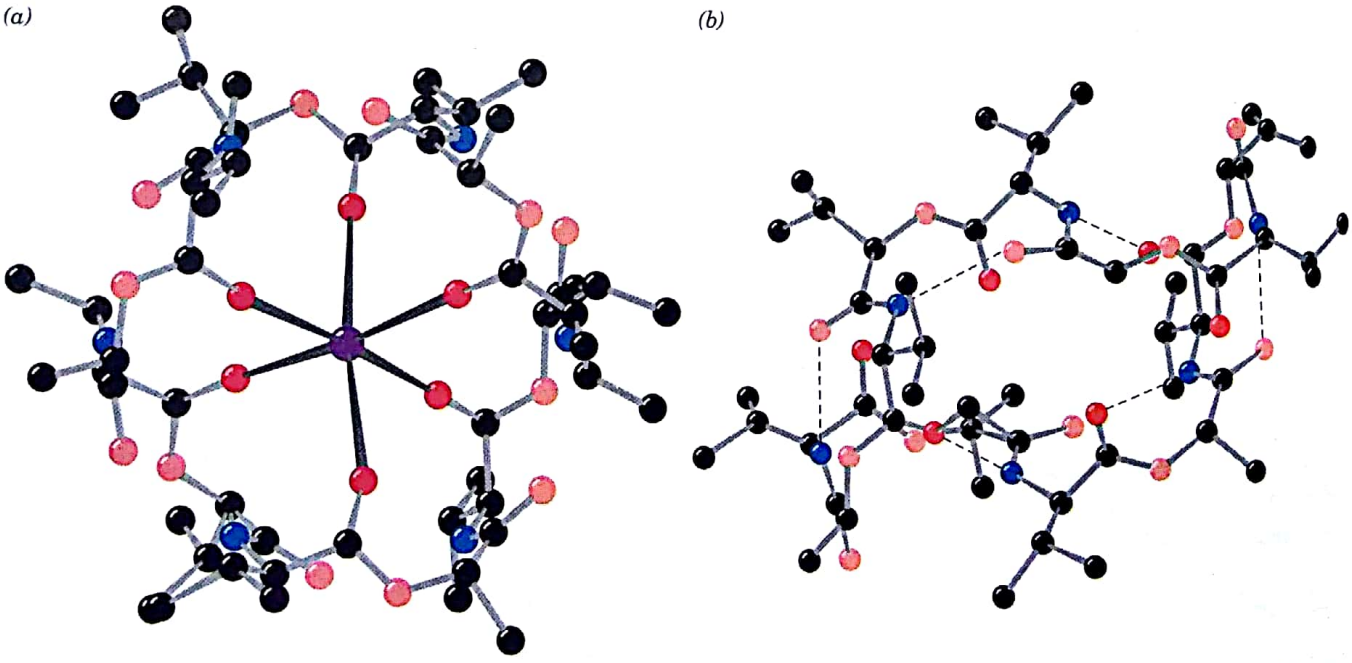


FIGURE 18-8. Valinomycin X-ray structures. (*a*) The K^+ complex. The six oxygen atoms that octahedrally complex the K^+ ion are darker red than the other oxygen atoms. [After Neupert-Laves, K. and Dobler, M., *Helv. Chim. Acta* **58**, 439 (1975).] (*b*) Uncomplexed valinomycin. [After Smith, G.D., Duax, W.L., Langs, D.A., DeTitta, G.T., Edmonds, R.C., Rohrer, D.C., and Weeks, C M., *J. Am. Chem. Soc.* **97**, 7242 (1975).] Hydrogen atoms are not shown.

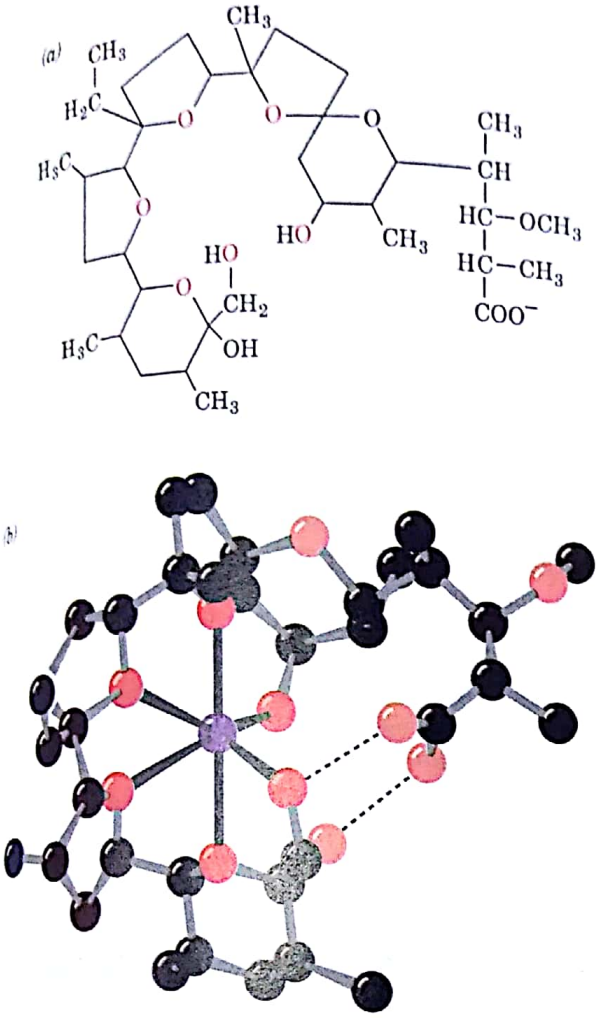


FIGURE 18-9. Monensin. (*a*) The structural formula with the six oxygen atoms that octahedrally complex Na^+ indicated in red. (*b*) The X-ray structure of the Na^+ complex (hydrogen atoms not shown). [After Duax, W.L., Smith, G.D., and Strong, P.D., *J. Am. Chem. Soc.* **102,** 6728 (1980).]

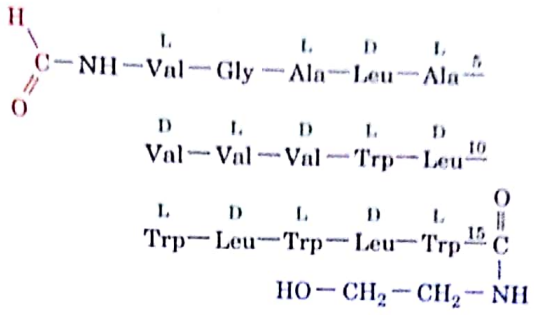


FIGURE 18-10. Gramicidin A consists of 15 alternating D- and L-amino acid residues and is blocked at both its N- and C-termini.

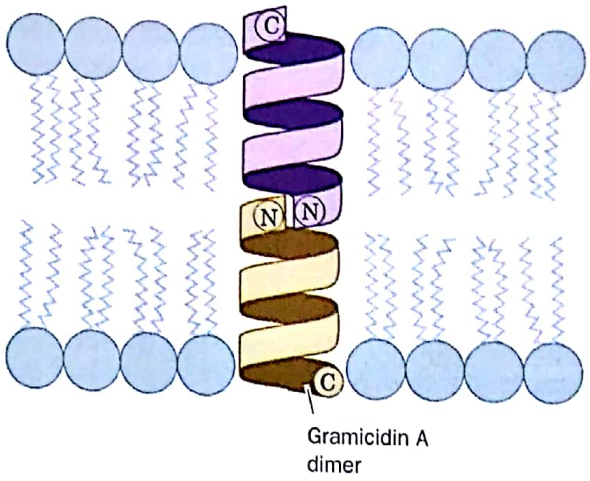


FIGURE 18-11. A schematic diagram of the transmembrane channel formed by two molecules of gramicidin A. The molecules presumably dimerize by a hydrogen bonding association between their *N*-formyl ends (N).

these ions with water are therefore energetically more favorable than their complexes with valinomycin. This accounts for valinomycin's 10,000-fold greater binding affinity for K^+ over Na^+. Indeed, no other known substance discriminates so acutely between Na^+ and K^+.

The Na^+-binding ionophore **monensin** (Fig. 18-9*a*), a linear polyether carboxylic acid, is chemically different from valinomycin. Nevertheless, X-ray analysis reveals that monensin's Na^+ complex has the same general features as valinomycin's K^+ complex in that monensin octahedrally coordinates Na^+ so as to wrap it in a nonpolar jacket (Fig. 18-9*b*). Other carrier ionophores have similar characteristics.

Gramicidin A Forms Helical Transmembrane Channels

Gramicidin A is a channel-forming ionophore from *Bacillus brevis* that permits the passage of protons and alkali cations but is blocked by Ca^{2+}. It is a 15-residue linear polypeptide of alternating L and D residues that is chemically blocked at its amino terminus by formylation and at its carboxyl terminus by an amide bond with ethanolamine (Fig. 18-10). Note that all of its residues are hydrophobic as is expected for a small transmembrane polypeptide. NMR and X-ray crystallographic evidence indicate that *gramicidin A dimerizes in a head-to-head fashion to form a transmembrane channel* (Fig. 18-11). This is corroborated by the observation that two gramicidin A molecules with their N-terminal amino groups covalently cross-linked form a functional ion channel.

The gramicidin A channel cannot be α helical because α helices lack a central channel and cannot consist of alternating L and D residues. Dan Urry has proposed that gramicidin A forms a novel helix that he named the **β helix** because it resembles a rolled up parallel β sheet. Successive backbone N—H groups in this model alternately point up and down the helix to hydrogen bond with backbone car-

bonyl groups. An NMR structure, by Timothy Cross, of gramicidin A in a lipid bilayer supports this model and shows that the helix is right handed with 6 to 7 residues per turn (Fig. 18-12). As a consequence of its alternating D and L residues, the side chains of the β helix festoon its periphery to form the channel's required hydrophobic exterior (recall that in a β sheet of all L-amino acid residues, the side chains alternately extend to opposite sides of the sheet; Section 7-1C). The polar backbone groups thus line the central channel and thereby facilitate the passage of ions. The four Trp side chains in the C-terminal half of each polypeptide chain are oriented with their polar N—H groups directed towards the bilayer surface, thereby orienting the dimeric helix perpendicular to the bilayer. Indeed, the replacement of these Trp residues by Phe significantly reduces the channel's conductivity without altering its backbone conformation.

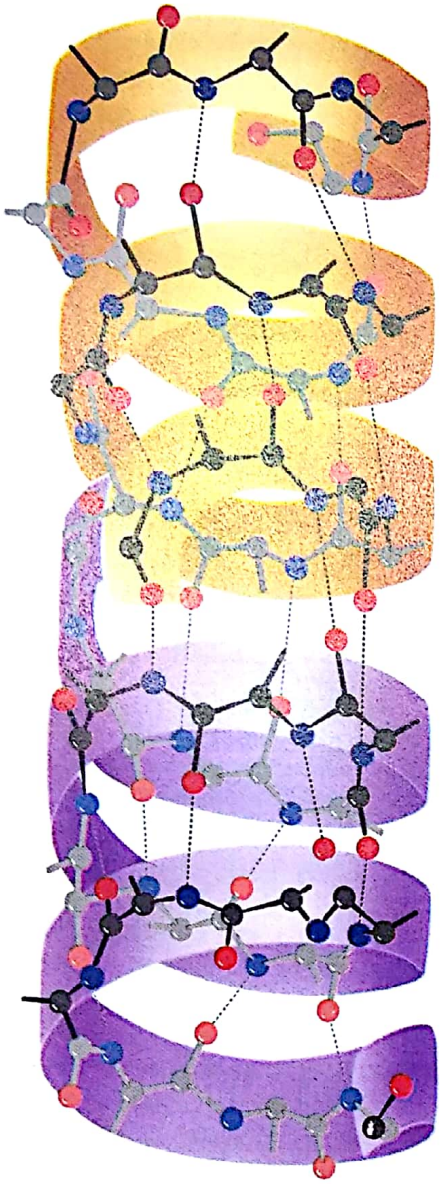


FIGURE 18-12. A model for the gramicidin A transmembrane channel. Each gramicidin A molecule of the head-to-head dimer forms a right-handed helix in which the hydrogen bonding pattern resembles that in a parallel β pleated sheet. The novel hydrogen bonding arrangement of this 26-Å-long "β helix" is made possible because the alternating D and L configurations of the amino acid residues permit both successive NH and successive CO groups to point in opposite directions along the helix. The helix's bore diameter of 4 Å is sufficient to permit passage of alkali metal cations. [After Dobler, M., *Ionophores and Their Structures, p.* 215, Wiley–Interscience (1981). Based on a model proposed by D.W. Urry.]

Porin Structures Explain Their Ion Selectivities

The only channel-forming proteins whose X-ray structures are presently known are the bacterial **porins**, trimeric transmembrane proteins, each of whose identical subunits consists mainly of a 16-stranded antiparallel β barrel that forms a solvent-accessible channel along its barrel axis (Section 11-3A). In the *E. coli* OmpF porin (Figs. 11-28 and 18-13), this ~50-Å-long channel is constricted near its center to an elliptical pore that has a minimum cross-section of 7 × 11 Å. Consequently, solutes of more than ~600 D are too large to pass through a porin channel. The OmpF porin is weakly cation selective, whereas the 63% identical *E. coli* PhoE porin is weakly anion selective. This

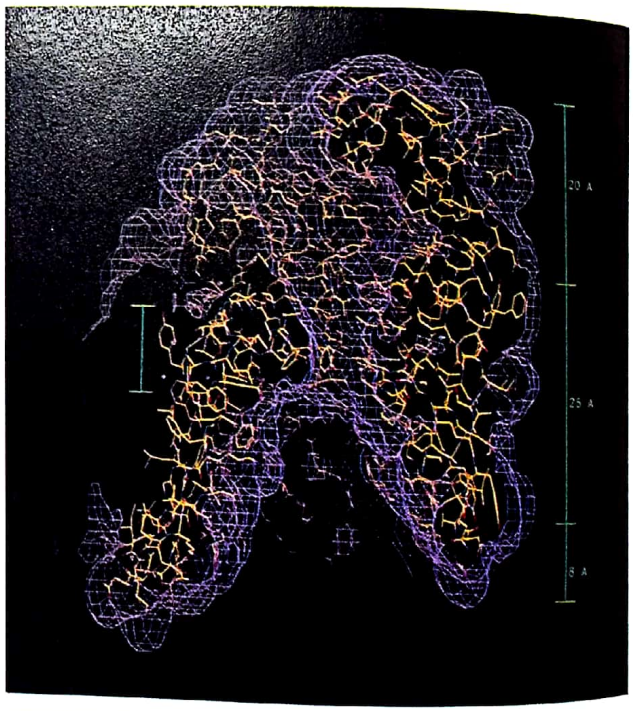


FIGURE 18-13. A longitudinal section through the pore of the OmpF porin subunit as seen in its X-ray structure. The meshwork indicates the protein's solvent-accessible surface (the part of the protein that is in contact with water). The narrowest part of the pore, which is ~9 Å in length, is indicated by the short vertical bar on the left. The vertical scale on the right is the same as that in Fig. 11-28*c* and, hence, reference to this figure indicates the position of the hydrophobic band on the exterior of the protein. [Courtesy of Tilman Schirmer and Johan Jansonius, University of Basel, Basel, Switzerland.]

difference in ion selectivity is largely explained by the presence of Lys 131 in PhoE, the homolog of Gly 131 in OmpF. The side chain of Lys 131 protrudes into the channel so as to extend a row of basic side chains lining one wall of the constriction zone. The mutagenic replacement of Lys 131 with Glu largely abolishes the anion selectivity of PhoE, whereas replacement of any of several Lys residues lining the mouth of the channel by Glu has a lesser effect on ion selectivity. Evidently, Lys 131 electrostatically facilitates the passage of anions, probably by providing an anion binding site, whereas it is likely that the Lys side chains at the mouth of the channel function to attract anions into the channel.

D. *Mechanism of Passive-Mediated Glucose Transport*

Integral membrane proteins either are exposed only at one surface of the membrane or, in the case of transmembrane proteins, are oriented in only one direction with respect to the membrane (Section 11-3A). Since protein flip-flop rates are negligible, *the mobile carrier model that describes the mechanism of ionophores such as valinomycin (Fig. 18-6a) is not applicable to protein-mediated transport; rather, some sort of channel or pore mechanism appears likely.*

Glucose Transport Occurs via a Gated Pore Mechanism

The erythrocyte glucose transporter is a 55-kD glycoprotein which, according to sequence hydropathy analysis (Sections 7-4C and 11-3A), has four major domains (Fig. 18-14): (1) a bundle of 12 membrane-spanning α helices that are thought to form a hydrophobic cylinder surrounding a hydrophilic channel through which the glucose is transported; (2) a large, highly charged, cytoplasmic domain located between helices 6 and 7; (3) a smaller, carbohydrate-bearing, external domain located between helices 1 and 2; and (4) a relatively large C-terminal domain which is also cytoplasmic. The glucose transporter accounts for 2% of erythrocyte membrane proteins and runs as band 4.5 in SDS-PAGE gels of erythrocyte membranes (Section 11-3C; it is not visible on the gel depicted in Fig. 11-34 because the heterogeneity of its oligosaccharide component makes the protein band diffuse).

Two observations support the hypothesis that the erythrocyte glucose transporter is asymmetrically disposed in the membrane (Fig. 18-14*b*):

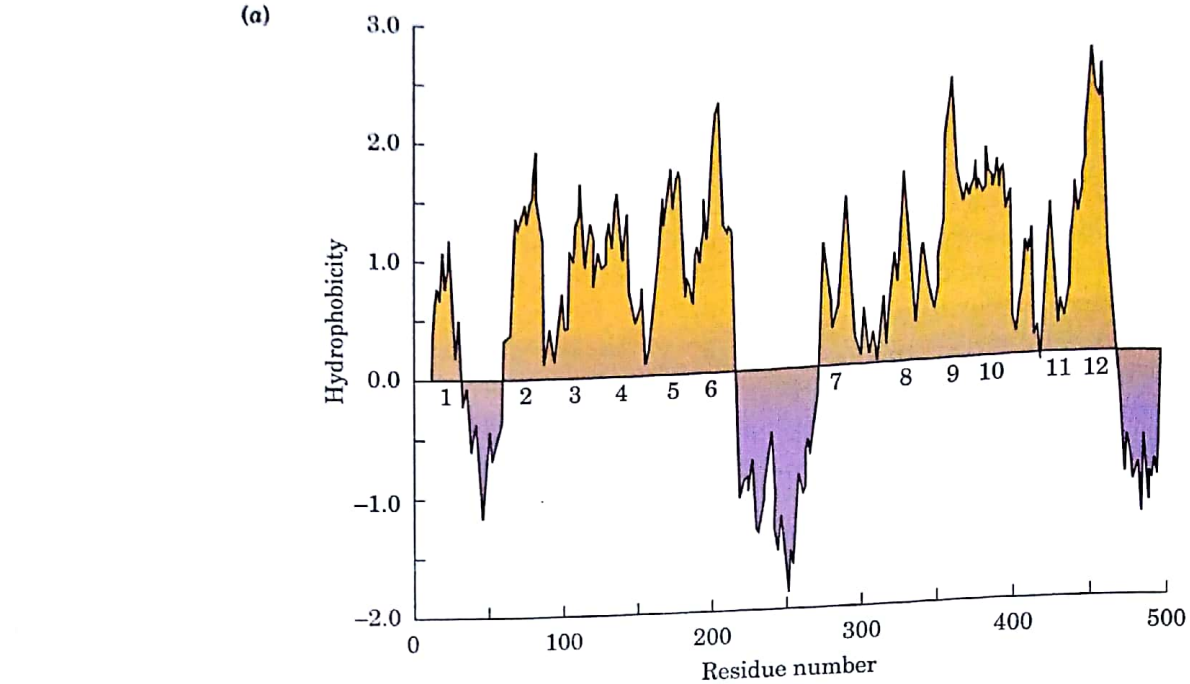
1. **Galactose oxidase** oxidizes the galactose units of the glucose transporter's carbohydrate moiety only when the oxidase is outside the erythrocyte. The transporter's galactose units must therefore be located on the erythrocyte cell surface.
2. Trypsin only disrupts glucose transport when it acts from within an erythrocyte ghost (erythrocytes made devoid of cytoplasm). The transporter's trypsin-sensitive amino acid residues must therefore be located only on the cytoplasmic surface of the erythrocyte plasma membrane.

The glucose-binding sites on the two sides of the erythrocyte membrane have different steric requirements as well. John Barnett showed that addition of a propyl group to glucose C1 prevents glucose binding to the outer surface of the membrane, whereas addition of a propyl group to C6 prevents binding to the inner surface. He therefore proposed that this transmembrane protein has two alternate conformations: one with the glucose site facing the external cell surface, requiring O1 contact, and leaving O6 free, and the other with the glucose site facing the internal cell surface, requiring O6 contact and leaving O1 free (Fig. 18-15). *Transport apparently takes place by binding glucose to the protein on one face of the membrane, followed by a conformational change that closes the first site while exposing the other.* Glucose can then dissociate from the protein having been translocated across the membrane. The transport cycle is completed by the reversion of the glucose transporter to its initial conformation in the absence of bound glucose. Since this cycle can occur in either direction, the direction of net glucose transport is from high to low glucose concentrations. The glucose transporter thereby provides a means of equilibrating the glucose concentration across the erythrocyte membrane without any accompanying leakage of small molecules or ions.

The mechanism of glucose transport across erythrocyte membranes is a general one, often referred to as a **gated pore.** Indeed, *all known transport proteins appear to be asymmetrically situated transmembrane proteins that alternate between two conformational states in which the ligand-binding sites are exposed, in turn, to alternate sides of the membrane.*

Eukaryotes Express a Variety of Glucose Transporters

The erythrocyte glucose transporter, known also as **GLUT1**, has a highly conserved amino acid sequence (98% sequence identity between humans and rats), which suggests that all segments of this protein are functionally significant. GLUT1 is expressed in most tissues, although in liver and muscle, tissues that are highly active in glucose transport, it is present in only tiny amounts. At least four other glucose transporters, **GLUT2** through **GLUT5**, are 40 to 65% identical to GLUT1 but have different tissue distributions. For example, GLUT2 is prominant in pancreatic β cells (which secrete insulin in response to increased [glucose]; Section 17-3F) and liver (where its defects result in Type I glycogen storage disease; Section 17-4), whereas **GLUT4** occurs mainly in muscle and fat cells. Note that the tissue distributions of these glucose transporters correlate with the response of these tissues to insulin: Liver is unresponsive to insulin (liver functions, in part, to maintain the level of blood glucose; Section 17-3F), whereas muscle and fat cells take up glucose when stimulated by insulin.


(a)
Hydrophobicity
3.0
2.0
1.0
0.0
−1.0
−2.0
0
100
200
300
400
500
Residue number
1
2
3
4
5
6
7
8
9
10
11
12

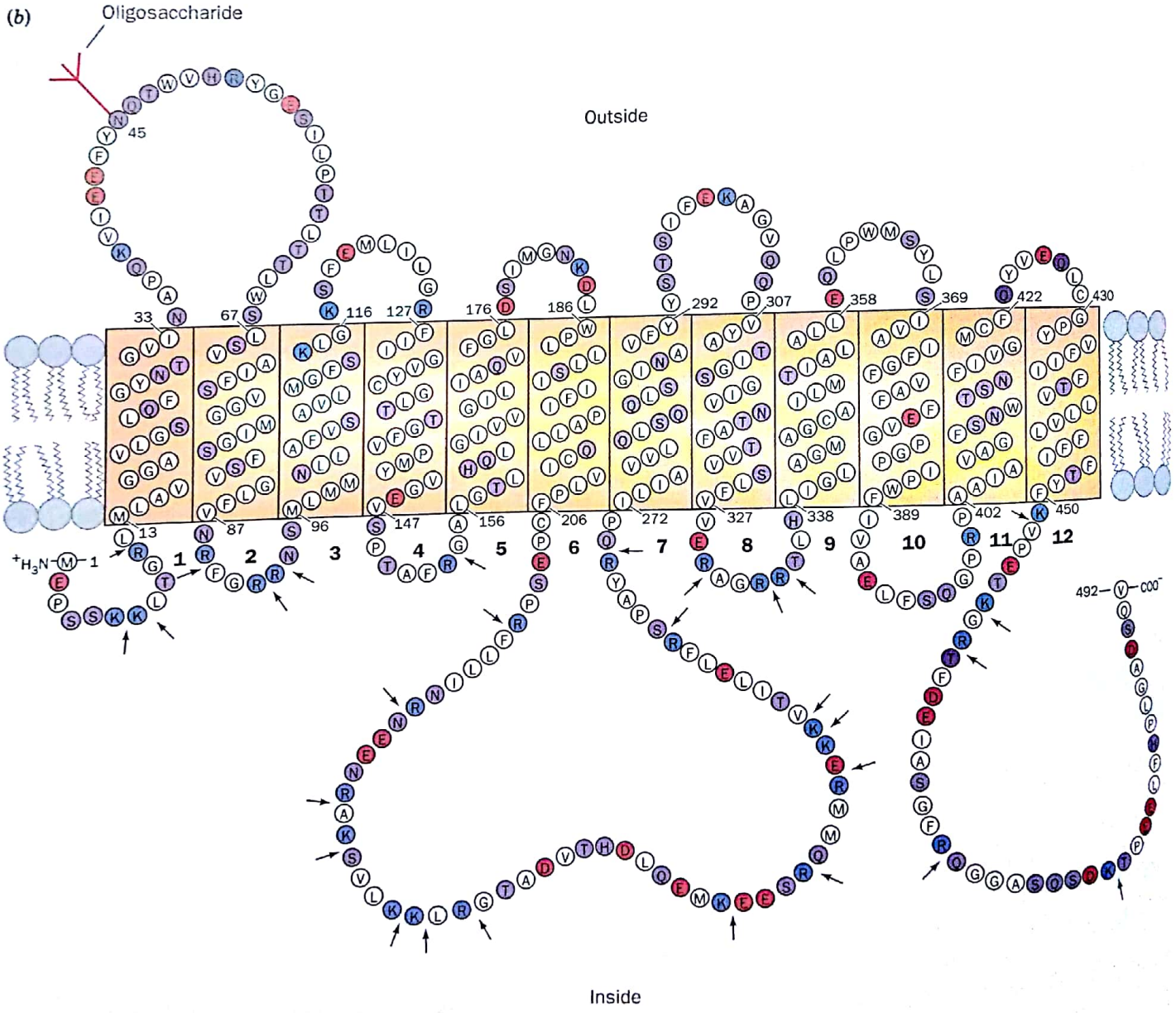

(b)
Oligosaccharide
Outside
Inside
$^{+}H_3N$–M–1
492–V–COO^{-}
1
2
3
4
5
6
7
8
9
10
11
12

FIGURE 18-14. (*Opposite*) (*a*) A hydropathy plot of the human erythrocyte glucose transporter amino acid sequence. The plot was generated by averaging the hydropathy values (Table 7-5) of the residues within a sliding window of 21 amino acid residues (enough to form a transmembrane α helix) and plotting these averages with respect to the position of the window's middle residue. The numbers refer to the 12 predicted membrane-spanning regions. [After Mueckler, M., Caruso, C., Baldwin, S.A., Panico, M., Blench, I., Morris, H.R., Allard, W.J., Lienhard, G.E., and Lodish, H.F., *Science*, **229**, 944 (1985).] (*b*) A predicted model for the orientation of the human erythrocyte glucose transporter in the erythrocyte membrane. Its amino acid sequence is given in terms of the one-letter code (Table 4-1) with positively charged residues (K and R) colored blue, negatively charged residues (D and E) colored red, and polar uncharged residues (H, N, Q, S, and T) colored purple. The numbered rectangles represent the 12 predicted membrane-spanning helices, each of which consists of precisely 21 residues. The predicted position of the *N*-linked oligosaccharide at Asp 45 is shown (the presumed site of galactose oxidase oxidation). Arrows point to potential tryptic cleavage sites. [After Davies, A., Ciardelli, T.L., Leinhard, G.E., Boyle, J.M., Whetton, A.D., and Baldwin, S.A., *Biochem. J.* **266**, 801 (1990).]

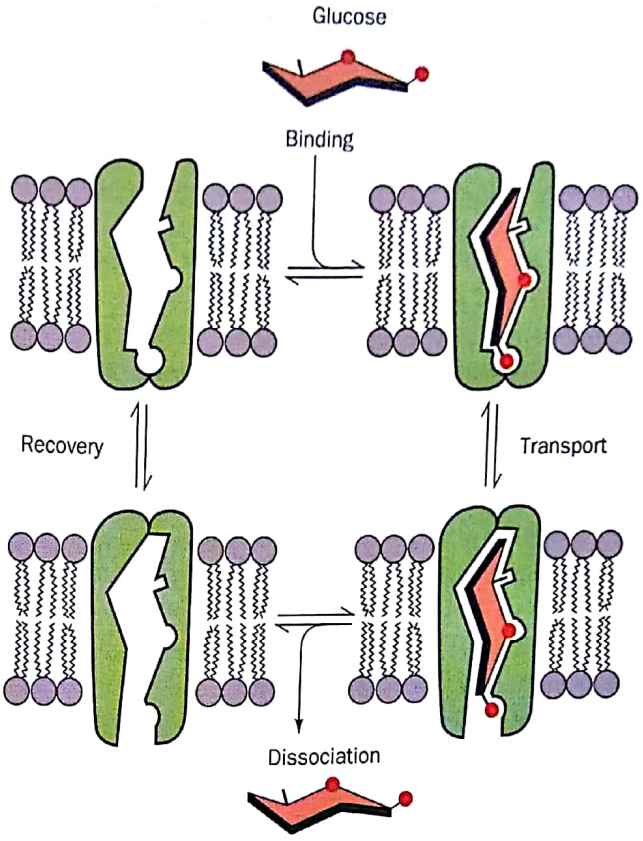


FIGURE 18-15. The alternating conformation model for glucose transport. Such a system is also known as a "gated pore." [After Baldwin, S.A., and Lienhard, G.E., *Trends Biochem. Sci.* **6**, 210 (1981).]

Cellular Glucose Uptake Is Regulated through the Insulin-Sensitive Exocytosis/Endocytosis of Glucose Transporters

Insulin stimulates fat and muscle cells to take up glucose. Within ~15 min after the administration of insulin, the J_{max} for passive-mediated glucose transport into these cells increases 6- to 12-fold, whereas the K_M remains constant. Upon withdrawal of the insulin, the rate of glucose uptake returns to its basal level within 20 min to 2 h depending on conditions. Neither the increase nor the decrease in the rate of glucose transport is affected by the presence of protein synthesis inhibitors so that these observations cannot be a consequence of the synthesis of new glucose transporter or of a protein that inhibits it. How, then, does insulin regulate glucose transport?

Basal state fat and muscle cells store most of their glucose transporters in internal membranous vesicles. Upon insulin stimulation, these vesicles fuse with the plasma membrane in a process known as ***exocytosis*** *(Fig. 18-16).* The consequent increased number of cell-surface glucose transporters (GLUT4) results in a proportional increase in the cell's glucose uptake rate. Upon insulin withdrawal, the process is reversed through the endocytosis of plasma membrane-embedded glucose transporters. The deletion or mutation

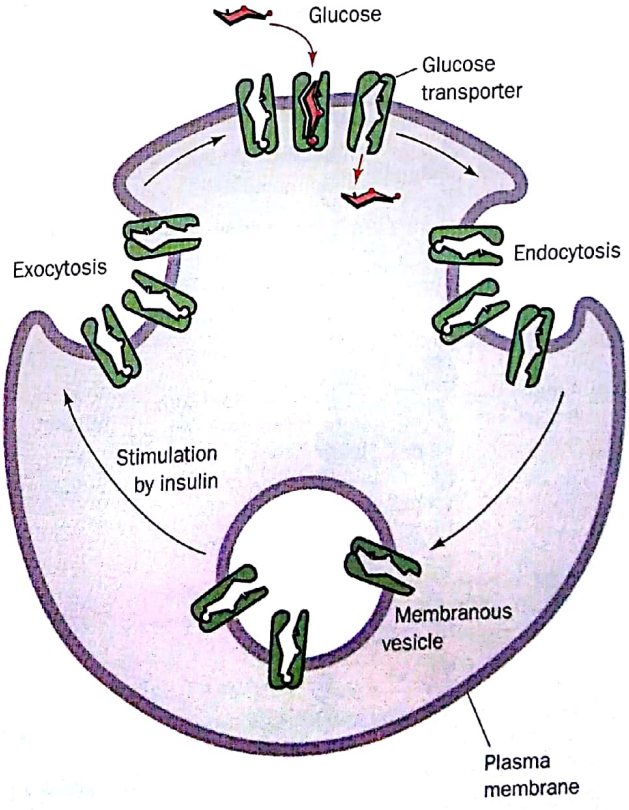


FIGURE 18-16. The regulation of glucose uptake in muscle and fat cells by the insulin-stimulated exocytosis (the opposite of endocytosis; Section 11-5C) of membranous vesicles containing GLUT4 glucose transporters (*left*). Upon insulin withdrawal, the process reverses itself through endocytosis (*right*).

of GLUT4's N-terminal eight residues, particulaly Phe 5, causes this transporter to accumulate in the plasma membrane. Evidently, GLUT4's N-terminal segment targets it for sequestration by the cell's endocytotic machinery, although how insulin controls this system is unknown.

3. ATP-DRIVEN ACTIVE TRANSPORT

Mediated transport is categorized according to the stoichiometry of the transport process (Fig. 18-17):

1. A **uniport** involves the movement of a single molecule at a time. The erythrocyte glucose transporter is a uniport system.
2. A **symport** simultaneously transports two different molecules in the same direction.
3. An **antiport** simultaneously transports two different molecules in opposite directions.

The electrical character of ion transport is further specified as:

1. **Electroneutral** (electrically silent) if there is simultaneous charge neutralization, either by symport of oppositely charged ions or antiport of similarly charged ions.
2. **Electrogenic** if the transport process results in a charge separation across the membrane.

Since the glucose concentration in blood plasma is generally higher than that in cells, the erythrocyte glucose transporter normally transports glucose into the erythrocyte,

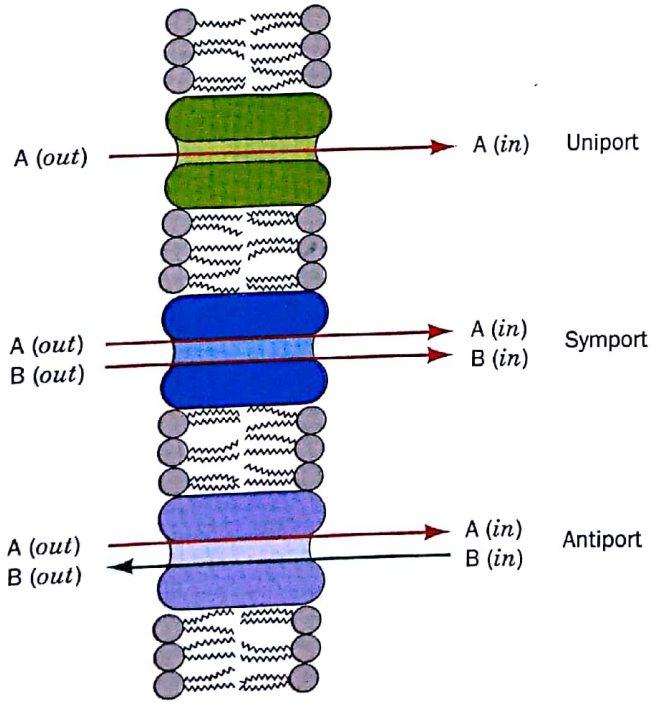


FIGURE 18-17. Uniport, symport, and antiport translocation systems.

where it is metabolized via glycolysis. Many substances, however, are available on one side of a membrane in lower concentrations than are required on the other side of the membrane. Such substances must be actively and selectively transported across the membrane against their concentration gradients.

Active transport is an endergonic process that is often coupled to the hydrolysis of ATP. How is this coupling accomplished? In endergonic biosynthetic reactions, it often occurs through the direct phosphorylation of a substrate by ATP; for example, the formation of UTP in the synthesis of glycogen (Section 17-2B). Membrane transport, however, is usually a physical rather than a chemical process; the transported molecule is not chemically altered. Determining the mechanism by which the free energy of ATP hydrolysis is coupled to endergonic physical processes has therefore been a challenging problem.

Three types of ATP hydrolyzing, transmembrane proteins have been identified that actively transport cations:

1. **P-type ATPases** are located mostly in plasma membranes and are directly phosphorylated by ATP during the transport process. They are distinguished from the other types of cation-translocating ATPases by their inhibition by **vandate** (VO_4^{3-}, a phosphate analog; see Problem 4 in this chapter).
2. **F-type ATPases (F_1F_0)** are located in mitochondria and are discussed in Section 20-3C.
3. **V-type ATPases** are located in plant vacuolar membranes and acidic vesicles, such as animal lysosomes, and are homologous to the F-type ATPases.

Anions are transported by a fourth type of ATPase, the so-called **A-type ATPase.** In this section, we discuss P-type ATPases. We also examine a bacterial active transport process in which the molecules transported are concomitantly phosphorylated. In the next section, we study secondary active transport systems, so-called because they utilize the free energy of electrochemical gradients generated by ion-pumping ATPases to transport ions and neutral molecules against their concentration gradients.

A. (Na^+–K^+)–ATPase of Plasma Membranes

One of the most thoroughly studied active transport systems is the **(Na^+–K^+)–ATPase** of plasma membranes. This transmembrane protein was first isolated in 1957 by Jens Skou. It consists of two types of subunits: A 110-kD nonglycosylated α subunit that contains the enzyme's catalytic activity and ion-binding sites, and an ~55-kD glycoprotein β subunit of unknown function. The sequences of the α subunits from several animal species, which are 98% identical in mammals, suggest that this subunit has around eight transmembrane α-helical segments and two large cytoplasmic domains. The β subunit is similarly predicted to have a single transmembrane helix and a large extracellular

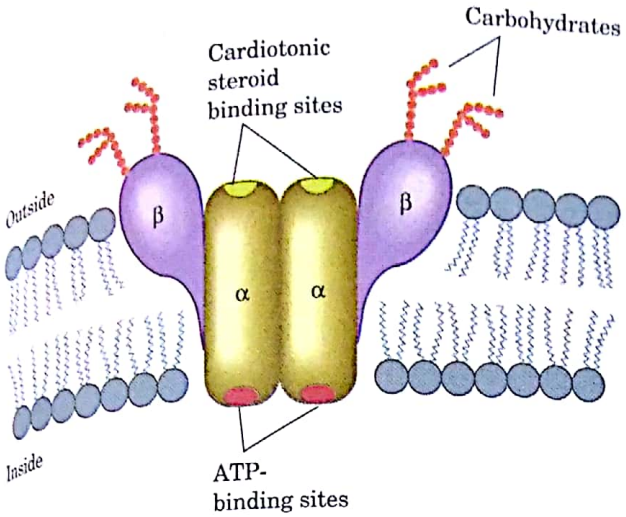


FIGURE 18-18. The putative dimeric structure of the (Na^+-K^+)-ATPase indicating its orientation in the plasma membrane.

domain. The protein is thought to have the subunit composition $(\alpha\beta)_2$ (Fig. 18-18), but it is unclear whether this dimeric structure is a functional necessity. The enzyme is often called the **(Na^+-K^+) pump** because *it pumps Na^+ out of and K^+ into the cell with the concomitant hydrolysis of intracellular ATP.* The overall stoichiometry of the (Na^+-K^+)-ATPase reaction is

$$3Na^+(in) + 2K^+(out) + ATP + H_2O \rightleftharpoons 3Na^+(out) + 2K^+(in) + ADP + P_i$$

The (Na^+-K^+)-ATPase is therefore an electrogenic antiport: Three positive charges exit the cell for every two that enter. This extrusion of Na^+ enables animal cells to control their water content osmotically; without functioning (Na^+-K^+) pumps, animal cells, which lack cell walls, would swell and burst (recall that lipid bilayers are permeable to H_2O; Section 11-2B). Moreover, the electrochemical potential gradient generated by the (Na^+-K^+) pump is responsible for the electrical excitability of nerve cells (Section 34-4C) and provides the free energy for the active transport of glucose and amino acids into some cells (Section 18-4A). In fact, *all cells expend a large fraction of the ATP they produce (up to 70% in nerve cells) to maintain their required cytosolic Na^+ and K^+ concentrations.*

ATP Phosphorylates an Essential Asp During the Transport Process

The free energy of ATP hydrolysis powers the endergonic transport of Na^+ and K^+ against an electrochemical gradient. In coupling these two processes, a kinetic barrier must somehow be erected against the "downhill" transport of Na^+ and K^+ along their ion concentration gradients, while simultaneously facilitating their "uphill" transport. In addition, futile ATP hydrolysis must be prevented in the absence of uphill transport. How the enzyme does so is by no means well understood, although many of its mechanistic aspects have been elucidated.

A key discovery was that the protein is phosphorylated by ATP in the presence of Na^+ during the transport process. The use of chemical trapping techniques demonstrated that this phosphorylation occurs on an Asp residue to form a highly reactive **aspartyl phosphate** intermediate. For instance, sodium borohydride reduces acyl phosphates to their corresponding alcohols. In the case of an aspartyl phosphate residue, the alcohol is homoserine. By use of $[^3H]NaBH_4$ to reduce the phosphorylated enzyme, radioactive homoserine was, in fact, isolated from the acid hydrolysate (Fig. 18-19).

The (Na^+-K^+)-ATPase Has Two Major Conformational States

The observations that ATP only phosphorylates the (Na^+-K^+)-ATPase in the presence of Na^+, while the aspartyl phosphate residue is only subject to hydrolysis in the presence of K^+, led to the realization that *the enzyme has two major conformational states, E_1 and E_2.* These states have different tertiary structures, different catalytic activities, and different ligand specificities:

1. E_1 has an inward-facing high-affinity Na^+-binding site ($K_M = 0.2$ mM, well below the intracellular $[Na^+]$) and reacts with ATP to form the activated product $E_1{\sim}P$ only when Na^+ is bound.

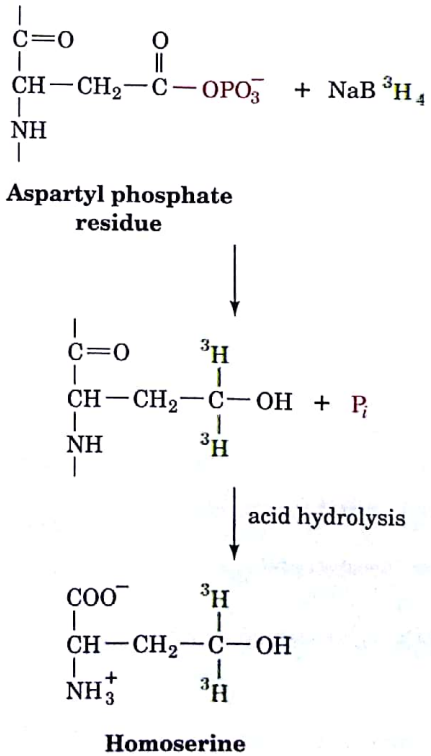


FIGURE 18-19. Reaction of $[^3H]NaBH_4$ with phosphorylated (Na^+-K^+)-ATPase. The isolation of $[^3H]$homoserine following acid hydrolysis of the protein indicates that the original phosphorylated amino acid residue is Asp.

2. E_2—P has an outward-facing high-affinity K^+-binding site ($K_M = 0.05M$, well below the extracellular $[K^+]$), and hydrolyzes to form $P_i + E_2$ only when K^+ is bound.

An Ordered Sequential Kinetic Reaction Mechanism Accounts for the Coupling of Active Transport with ATP Hydrolysis

The (Na^+-K^+)–ATPase is thought to operate in accordance with the following ordered sequential reaction scheme (Fig. 18-20):

1. $E_1 \cdot 3Na^+$, which acquired its Na^+ inside the cell, binds ATP to yield the ternary complex $E_1 \cdot ATP \cdot 3Na^+$.
2. The ternary complex reacts to form the "high-energy" aspartyl phosphate intermediate $E_1 \sim P \cdot 3Na^+$.
3. This "high-energy" intermediate relaxes to its "low-energy" conformation, E_2—$P \cdot 3Na^+$, and releases its bound Na^+ outside the cell, that is, Na^+ is transported through the membrane.
4. E_2—P binds $2K^+$ from outside the cell to form E_2—$P \cdot 2K^+$.
5. The phosphate group is hydrolyzed yielding $E_2 \cdot 2K^+$.
6. $E_2 \cdot 2K^+$ changes conformation, releases its $2K^+$ inside the cell, and replaces it with $3Na^+$, thereby completing the transport cycle.

The enzyme is thought to have only one set of cation-binding sites, which apparently changes both its orientation and its specificity during the course of the transport cycle.

The obligatory order of the reaction requires that ATP can be hydrolyzed only as Na^+ is transported "uphill." Conversely, Na^+ can be transported "downhill" only if ATP is concomitantly synthesized. Consequently, although each of the above reaction steps is, in fact, individually reversible, the cycle, as is diagrammed in Fig. 18-20, circulates only in the clockwise direction under normal physiological conditions; that is, ATP hydrolysis and ion transport are coupled processes. Note that the vectorial (unidirectional) nature of the reaction cycle results from the alternation of some of the steps of the exergonic ATP hydrolysis reaction (Steps 1+2 and Step 5) with some of the steps of the endergonic ion transport process (Steps 3+4 and Step 6). Thus, neither reaction can go to completion unless the other one also does.

Mutual Destabilization Accounts for the Rate of Na^+ and K^+ Transport

The above ordered kinetic mechanism accounts only for the coupling of active transport with ATP hydrolysis. *In order to maintain a reasonable rate of transport, the free energies of all its intermediates must be roughly equal. If some intermediates were much more stable than others, the stable intermediates would accumulate, thereby severely reducing the overall transport rate.* For example, in order for Na^+ to be transported out of the cell, uphill, its binding to E_1 must be strong on the inside and weak to E_2 on the outside. Strong binding means greater stability and a potential bottleneck. This difficulty is counteracted by the phosphorylation of $E_1 \cdot 3Na^+$ and its subsequent conformational change to yield the low Na^+ affinity E_2—P (Steps 2 and 3, Fig. 18-20). Likewise, the strong binding of K^+ to E_2—P on the outside is attenuated by its dephosphorylation and conformational change to yield the low K^+ affinity E_1 (Steps 5 and 6, Fig. 18-20). It is these mutual destabilizations that permit Na^+ and K^+ to be transported at a rapid rate.

Cardiac Glycosides Specifically Inhibit the (Na^+-K^+)-ATPase

Study of the (Na^+-K^+)–ATPase has been greatly facilitated by the use of **cardiac glycosides** (also called cardio-

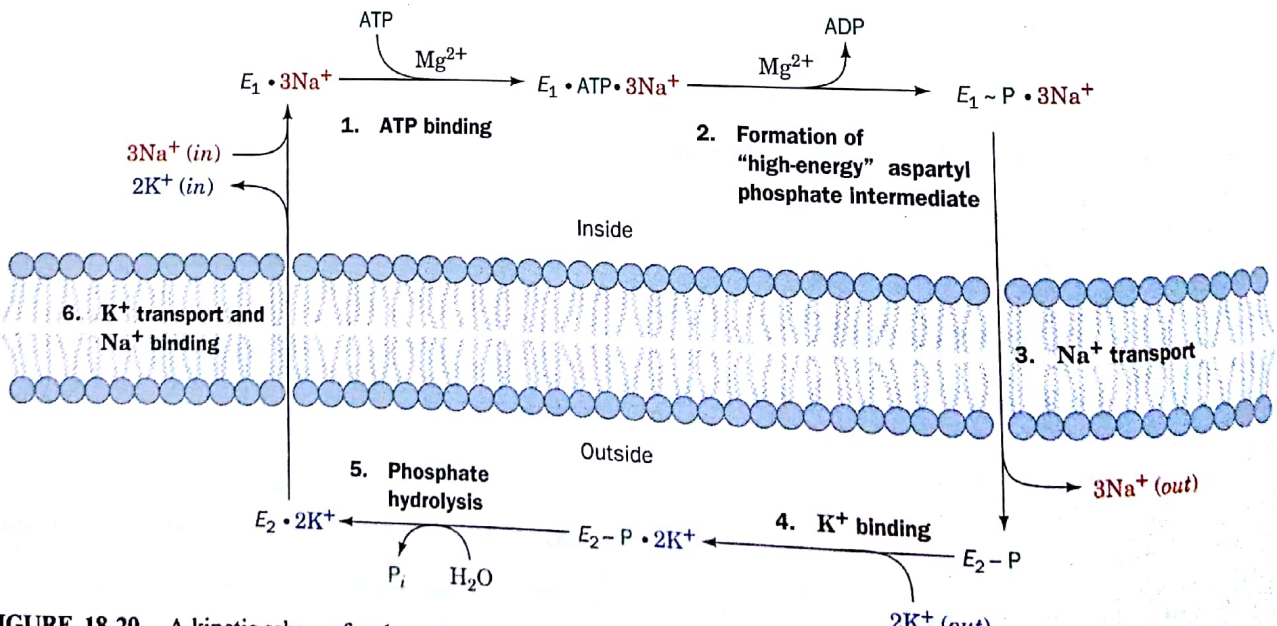
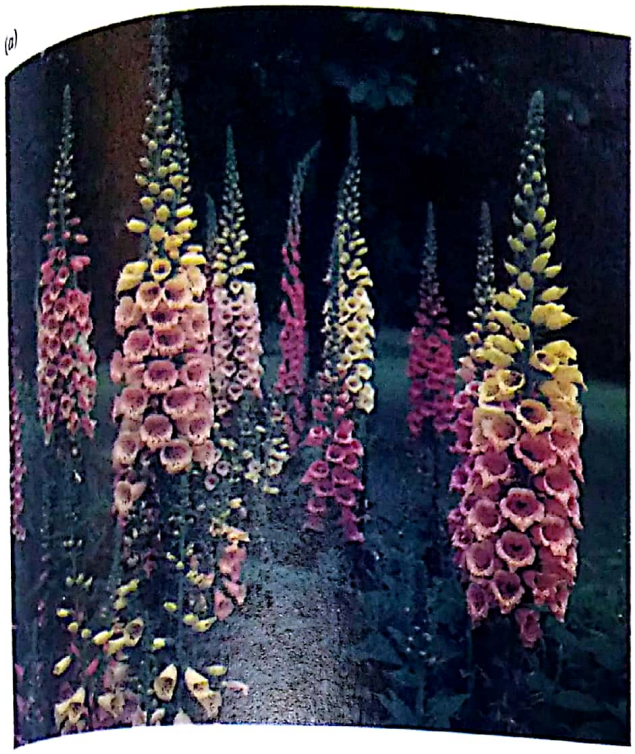
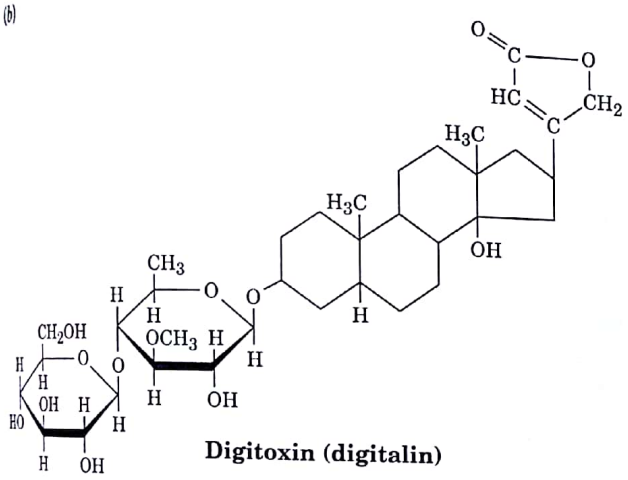


FIGURE 18-20. A kinetic scheme for the active transport of Na^+ and K^+ by (Na^+-K^+)–ATPase.

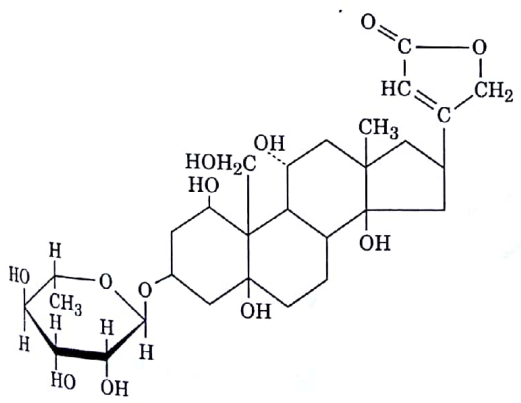
(a)



(b)



Digitoxin (digitalin)



Ouabain

FIGURE 18-21. (*a*) The leaves of the purple foxglove plant are the source of the heart muscle stimulant digitalis. [Derek Fell.] (*b*) Digitoxin (digitalin), the major component of digitalis; and ouabain, a cardiac glycoside isolated from the East African Ouabio tree, are among the most commonly prescribed cardiac drugs.

tonic steroids), natural products that increase the intensity of heart muscle contraction. Indeed, **digitalis**, an extract of purple foxglove leaves (Fig. 18-21*a*), which contains a mixture of cardiac glycosides including **digitoxin (digitalin;** Fig. 18-21*b*), has been used to treat congestive heart failure for centuries. The cardiac glycoside **ouabain** (pronounced wabane; Fig. 18-21*b*), a product of the East African Ouabio tree, has been long used as an arrow poison. These two steroids, which are still among the most commonly prescribed cardiac drugs, inhibit the (Na^+-K^+)-ATPase by binding strongly to an externally exposed portion of the enzyme (the drugs are ineffective when injected inside cells) so as to block Step 5 in Fig. 18-20. The resultant increase in intracellular $[Na^+]$ stimulates the cardiac (Na^+-Ca^{2+}) antiport system, which pumps Na^+ out of and Ca^{2+} into the cell (Section 20-1B). The increased cytosolic $[Ca^{2+}]$ boosts the $[Ca^{2+}]$ in other cellular organelles, principally the sarcoplasmic reticulum. Thus, the release of Ca^{2+} to trigger muscle contraction (Section 34-3C) produces a larger than normal increase in cytosolic $[Ca^{2+}]$, thereby intensifying the force of cardiac muscle contraction. Ouabain, which was once thought to be produced only by plants, has recently been discovered also to be an animal hormone that is secreted by the adrenal cortex and functions to regulate cell $[Na^+]$ and overall body salt and water balance.

B. Ca^{2+}-ATPase

Ca^{2+} often acts as a second messenger in a manner similar to cAMP. Transient increases in cytosolic $[Ca^{2+}]$ trigger numerous cellular responses, including muscle contraction (Section 34-3C), release of neurotransmitters (Section 34-4C), and, as we have seen, glycogen breakdown (Section 17-3C). Moreover, Ca^{2+} is an important activator of oxidative metabolism (Section 19-4).

The use of phosphate as a basic energy currency requires cells to maintain a low internal $[Ca^{2+}]$ because, for example, $Ca_3(PO_4)_2$ has a maximum aqueous solubility of 65 μM. Thus, the $[Ca^{2+}]$ in the cytosol (~0.1 μM) is four orders of magnitude less than it is in the extracellular spaces (~1500 μM). This large concentration gradient is maintained by the active transport of Ca^{2+} across the plasma membrane, the endoplasmic reticulum (the sarcoplasmic reticulum in muscle), and the mitochondrial inner membrane. We discuss the mitochondrial system in Section 20-1B. Plasma membrane and endoplasmic reticulum each contain a P-type **Ca^{2+}-ATPase (Ca^{2+} pump)** that actively pumps Ca^{2+} out of the cytosol at the expense of ATP hydrolysis. Their kinetic mechanisms (18-22) are very similar to that of the (Na^+-K^+)-ATPase (Fig. 18-20).

Calmodulin Regulates the Plasma Membrane Ca^{2+} Pump

For a cell to maintain its proper physiological state, it must regulate the activities of its ion pumps precisely. *The regulation of the Ca^{2+} pump in the plasma membrane is controlled by the level of Ca^{2+} through the mediation of*

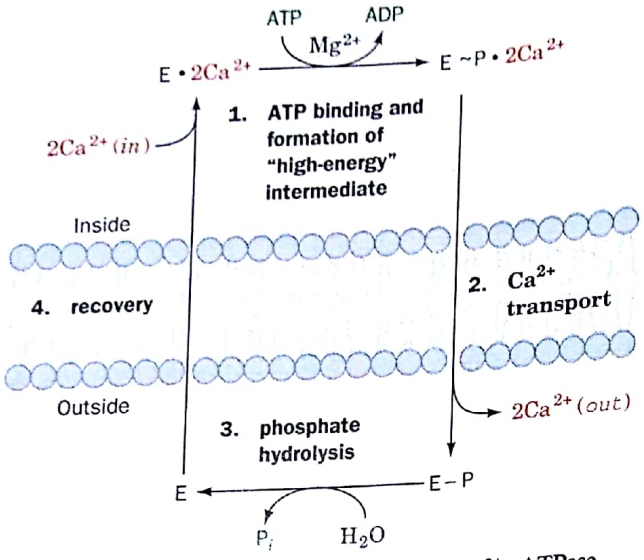


FIGURE 18-22. The kinetic mechanism of Ca^{2+}–ATPase. Here (*in*) refers to the cytosol and (*out*) refers to the outside of the cell for plasma membrane Ca^{2+}–ATPase or the lumen of the endoplasmic reticulum (sarcoplasmic reticulum) for the Ca^{2+}–ATPase of that membrane.

calmodulin (CaM). This ubiquitous eukaryotic Ca^{2+}-binding protein participates in numerous cellular regulatory processes including, as we have seen, the control of glycogen metabolism (Section 17-3C).

Ca^{2+}–Calmodulin activates the Ca^{2+}–ATPase of plasma membranes. The activation, as deduced from the study of the isolated ATPase, results in a decrease in its K_M for Ca^{2+} from 20 to 0.5 μM. Ca^{2+}–CaM activates the Ca^{2+} pump by binding to an inhibitory polypeptide segment of the pump in a manner similar to the way in which Ca^{2+}–CaM activates its target protein kinases (Section 17-3C). Evidence supporting this mechanism comes from proteolytically excising the Ca^{2+} pump's CaM-binding polypeptide, yielding a truncated pump that is active even in the absence of CaM. Synthetic peptides corresponding to this CaM-binding domain not only bind Ca^{2+}–CaM but inhibit the truncated pump by increasing its K_M for Ca^{2+} and decreasing its V_{max}. This suggests that, in the absence of Ca^{2+}–CaM, the CaM-binding domain of the pump interacts with the rest of the protein so as to inhibit its activity. When the Ca^{2+} concentration increases, Ca^{2+}–CaM forms and binds to the CaM-binding domain of the pump in a way that causes it to dissociate from the rest of the pump, thereby relieving the inhibition.

Now we can see how Ca^{2+} regulates its own cytoplasmic concentration: At Ca^{2+} levels below calmodulin's ~1-μM dissociation constant for Ca^{2+}, the Ca^{2+}–ATPase is relatively inactive due to autoinhibition by its CaM-binding domain. If, however, the [Ca^{2+}] rises to this level, Ca^{2+} binds to calmodulin which, in turn, binds to the CaM-binding domain so as to relieve the inhibition, thereby activating the Ca^{2+} pump:

$$Ca^{2+} + CaM \rightleftharpoons Ca^{2+}\text{–}CaM^* + \text{pump } (\textit{inactive}) \rightleftharpoons Ca^{2+}\text{–}CaM^*\cdot\text{pump } (\textit{active})$$

(CaM^* indicates activated calmodulin). This interaction decreases the pump's K_M for Ca^{2+} to below the ambient [Ca^{2+}], thereby causing Ca^{2+} to be pumped out of the cytosol. When the [Ca^{2+}] decreases sufficiently, Ca^{2+} dissociates from calmodulin and this series of events reverses itself, thereby inactivating the pump. The entire system is therefore analogous to a basement sump pump that is automatically activated by a float when the water reaches a preset level.

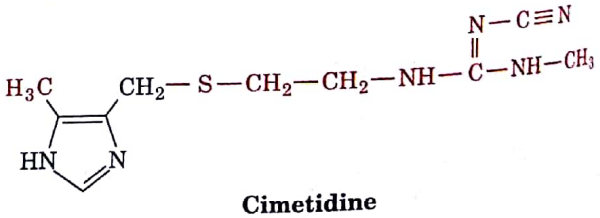
C. $(H^+–K^+)$–ATPase of Gastric Mucosa

Parietal cells of the mammalian gastric mucosa secrete HCl at a concentration of 0.15M (pH 0.8). Since the cytosolic pH of these cells is 7.4, this represents a pH difference of 6.6 units, the largest known in eukaryotic cells. The secreted protons are derived from the intracellular hydration of CO_2 by carbonic anhydrase:

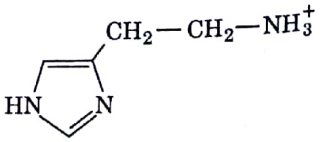
$$CO_2 + H_2O \rightleftharpoons HCO_3^- + H^+$$

The secretion of H^+ involves the participation of an **(H^+–K^+)–ATPase,** an electroneutral antiport with structure and properties similar to that of (Na^+–K^+)–ATPase. Like the related (Na^+–K^+)– and Ca^{2+}–ATPases, it is phosphorylated during the transport process. In this case, however, the K^+, which enters the cell as H^+ is pumped out, is subsequently externalized by its electroneutral cotransport with Cl^-. HCl is therefore the overall transported product.

For many years, effective treatment of peptic ulcers, which was a frequently fatal condition caused by the attack of stomach acid on the gastric mucosa, often required the surgical removal of the affected portions of the stomach. The discovery, by James Black, of **cimetidine,**



Cimetidine



Histamine

which inhibits stomach acid secretion, has almost entirely eliminated the need for this dangerous and

debilitating surgery. The (H^+-K^+)-ATPase of the gastric mucosa is activated by histamine stimulation of a cell-surface receptor in a process mediated by cAMP. Cimetidine (trade name: Tagamet) and its analogs, which competitively inhibit the binding of histamine to this receptor, are presently among the most commonly prescribed drugs in the United States.

D. Group Translocation

Group translocation is a variation of ATP-driven active transport that most bacteria use to import certain sugars. It is required for many bacterial processes, both useful and harmful (to humans), such as those that produce cheese, soy sauce, and dental cavities. *It differs from active transport in that the molecules transported are simultaneously modified chemically.* The most extensively studied example of group translocation is the **phosphoenolpyruvate-dependent phosphotransferase system (PTS)** of *E. coli* discovered by Saul Roseman in 1964. Phosphoenolpyruvate (PEP) is the phosphoryl donor for this system (recall that PEP is the "high-energy" phosphoryl donor for ATP synthesis in the pyruvate kinase reaction of glycolysis; Section 16-2J). *The PTS simultaneously transports and phosphorylates sugars. Since the cell membrane is impermeable to sugar phosphates, once they enter the cell, they remain there.* Some of the PTS-transported sugars are listed in Table 18-2.

TABLE 18-2. SOME OF THE SUGARS TRANSPORTED BY THE *E. COLI* PEP-DEPENDENT PHOSPHOTRANSFERASE SYSTEM (PTS)

Glucose	Galactitol
Fructose	Mannitol
Mannose	Sorbitol
N-Acetylglucosamine	Xylitol

The PTS system involves two soluble cytoplasmic proteins, **Enzyme I (E I)** and **HPr** (for histidine-containing phosphocarrier protein), which participate in the transport of all sugars (Fig. 18-23). In addition, for each sugar the system transports, there is a specific transmembrane transport protein **E II,** and in some cases, a sugar-specific protein **E III** that is membrane bound for some sugars and cytoplasmic for others. Glucose transport, for example, requires the participation of **E II**^{glc} and **E III**^{glc}.

Glucose transport, which resembles that of other sugars, involves the transfer of a phosphoryl group from PEP to glucose with net inversion of configuration about the phosphorus atom. Since each phosphoryl transfer involves inversion (Section 15-2B), an odd number of transfers must be involved. Four phosphorylated protein intermediates have been identified, indicative of five phosphoryl transfers:

$$\text{PEP} \rightarrow \text{E I} \rightarrow \text{HPr} \rightarrow \text{E III}^{glc} \rightarrow \text{E II}^{glc} \rightarrow \text{glucose}$$

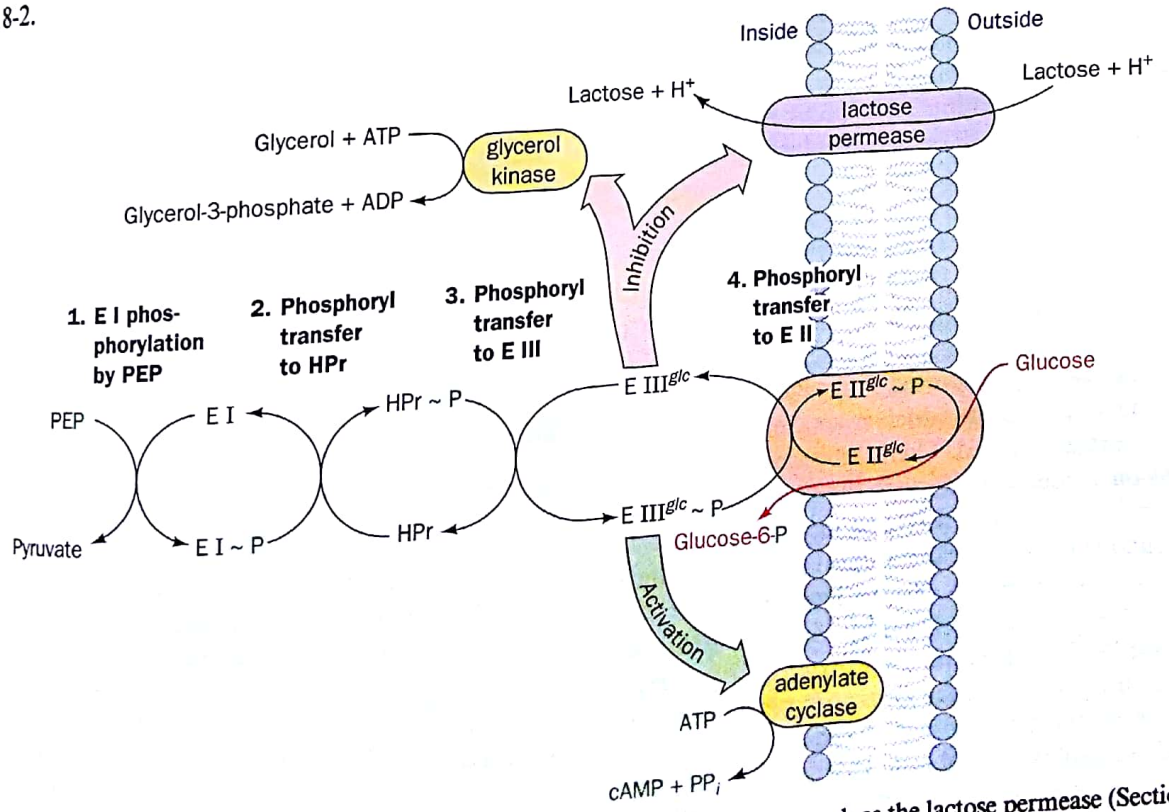
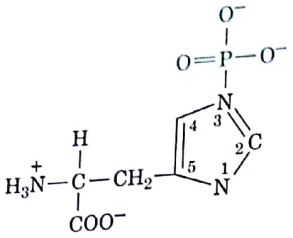


FIGURE 18-23. Transport of glucose by the PEP-dependent phosphotransferase system (PTS). HPr and E I are cytoplasmic proteins common to all sugars transported. E II^{glc} and E III^{glc} are proteins specific for glucose. E III^{glc} inhibits non-PTS transport proteins such as the lactose permease (Section 18-4B) and enzymes such as glycerol kinase. Adenylate cyclase is activated by the presence of E III^{glc}~P (or possibly inhibited by the presence of E III^{glc}).

The transport process occurs as follows (Fig. 18-23):

1. PEP phosphorylates E I at N3 of His 189 to form a reactive phosphohistidine adduct.



Phosphohistidine

2. The phosphoryl group is transferred to N1 of His 15 on HPr. His is apparently a favored phosphoryl group acceptor in phosphoryl transfer reactions. It also participates in the phosphoglycerate mutase reaction of glycolysis (Section 16-2H).
3. HPr~P continues the phosphoryl-transfer chain by phosphorylating E III^{glc}, again on a His residue, His 90.
4. The fourth phosphoryl transfer is to Cys 421 of E II^{glc}.
5. The phosphoryl group is finally transferred from E II^{glc} to glucose, which, in the process, is transported across the membrane by E II^{glc}. Glucose is released into the cytoplasm only after it has been phosphorylated to glucose-6-phosphate (G6P).

Thus the transport of glucose is driven by its indirect, exergonic phosphorylation by PEP. The PTS is an energy-efficient system since only one ATP-equivalent is required to both transport and phosphorylate glucose. When the active transport and phosphorylation steps occur separately, as they do in many cells, two ATPs are hydrolyzed per glucose processed.

Bacterial Sugar Transport Is Genetically Regulated

The PTS is more complex than the other transport systems we have encountered, probably because it is part of a complicated regulatory system governing sugar transport. When any of the sugars transported by the PTS is abundant, the active transport of sugars which enter the cell via other transport systems is inhibited. This inhibition, called **catabolite repression,** is mediated through the cAMP concentration (Section 29-3C). cAMP activates the transcription of genes that encode various sugar transport proteins, including **lactose permease** (Section 18-4B). The presence of glucose results in a decrease in [cAMP] which, in turn, represses the synthesis of these other sugar transport proteins. Direct inhibition of the sugar transport proteins themselves, as well as of certain enzymes, also occurs.

The mechanism for control of [cAMP] is thought to reside in E III^{glc}, which is transiently phosphorylated in Step 3 of the PTS transport process (Fig. 18-23). When glucose is plentiful, this enzyme is present mostly in its dephospho form since E III^{glc}~P rapidly transfers its phosphoryl group through to glucose. Under these conditions, adenylate cyclase is inactive, although whether dephospho E III^{glc} inhibits this enzyme or E III^{glc}~P activates it is unclear. However, dephospho E III^{glc} binds to and inhibits many non-PTS transporters and enzymes that participate in the the metabolism of sugars other than glucose (the metabolite of choice for many bacteria), including lactose permease and glycerol **kinase** (Section 16-5). In the absence of glucose, E III^{glc} is converted to E III^{glc}~P, thereby relieving the inhibition of non-PTS transporters. In addition, adenylate cyclase is activated to produce cAMP, which, in turn, induces the increased production of some of the non-PTS transporters and enzymes that E III^{glc} inhibits. This is a form of energy conservation for the cell. Why synthesize the proteins required for the transport and metabolism of all sugars when the metabolism of only one sugar at a time will do?

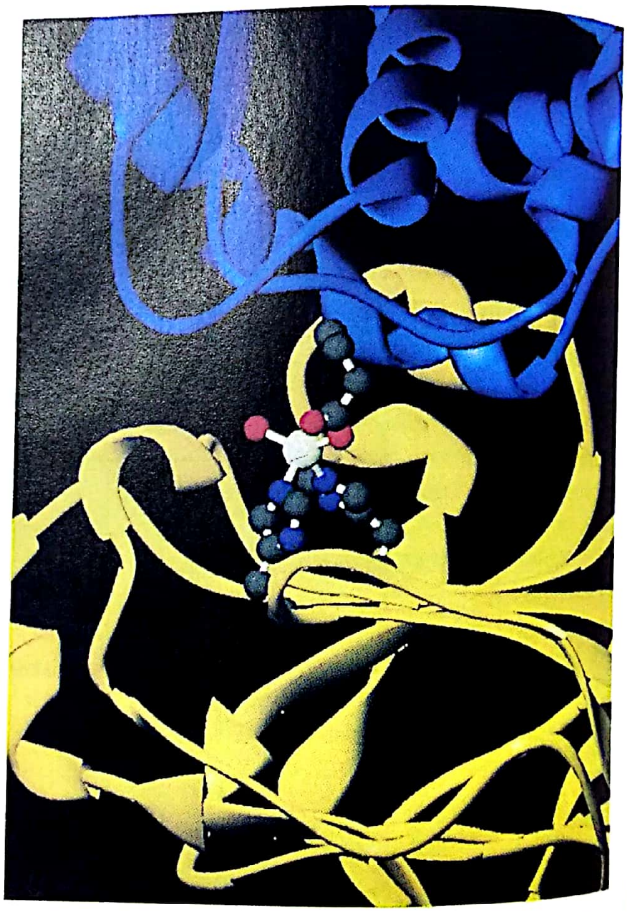


FIGURE 18-24. The X-ray structure of *E. coli* E III^{glc} (*yellow*, a 168-residue monomer) in complex with one of its regulatory targets, glycerol kinase (*blue*, a tetramer of identical 501-residue subunits). The two proteins associate, in part, by tetrahedrally coordinating a Zn^{2+} ion via the side chains of His 75 and His 90 of E III^{glc}, a carboxylate oxygen from Glu 478 of glycerol kinase, and a water molecule. These groups are shown in ball-and-stick form with C grey, N blue, O red, and Zn^{2+} white. The Zn^{2+}-mediated interaction between E III^{glc} and glycerol kinase inactivates glycerol kinase, presumably through an induced fit mechanism. The phosphorylation of E III^{glc} at His 90 disrupts this interaction, thereby reversing the inhibition of glycerol kinase. [Courtesy of James Remington, University of Oregon.]

The X-Ray Structure of E III^{glc} in Complex with Glycerol Kinase

The X-ray structures of E III^{glc}, both alone and in complex with one of its regulatory targets, glycerol kinase, which were determined by James Remington and Rosemarin, have revealed how E III^{glc} inhibits at least some of its targets and why E III^{glc}~P does not do so. E III^{glc} contains two His residues, His 75 and His 90, that are required for phosphoryl transfer, although only His 90 is necessary for E III^{glc} to accept a phosphate from HPr. The X-ray structure of *E. coli* E III^{glc} alone reveals that these two His residues lie in close proximity (their N3 atoms are 3.3 Å apart) in a depression on the surface of the protein that is surrounded by a remarkable ~18-Å in diameter hydrophobic ring consisting of 11 Phe, Val, and Ile side chains.

The X-ray structure of E III^{glc} in complex with glycerol kinase (Fig. 18-24) confirms that this hydrophobic gasket is indeed the site of interaction between the two proteins and reveals how the phosphorylation of His 90 disrupts this interaction. The two active site His residues, which are completely buried within the hydrophobic interaction surface, coordinate with a previously unanticipated Zn^{2+} ion, which is additionally coordinated to Glu 478 of glycerol kinase and a water molecule. The phosphorylation of E III^{glc} His 90 to yield E III^{glc}~P no doubt disrupts this intermolecular interaction, thereby releasing glycerol kinase and reversing its inhibition.

4. ION GRADIENT–DRIVEN ACTIVE TRANSPORT

Systems such as the $(Na^+–K^+)$–ATPase discussed above utilize the free energy of ATP hydrolysis to generate electrochemical potential gradients across membranes. Conversely, *the free energy stored in an electrochemical potential gradient may be harnessed to power various endergonic physiological processes.* Indeed, ATP synthesis by mitochondria and chloroplasts is powered by the dissipation of proton gradients generated through electron transport and photosynthesis (Sections 20-3C and 22-2D). In this section we discuss active transport processes that are driven by the dissipation of ion gradients. We consider three examples: intestinal uptake of glucose by the **Na^+–glucose symport,** uptake of lactose by *E. coli* ***lactose permease,*** *and the mitochondrial* ***ADP–ATP transporter.***

A. Na^+–Glucose Symport

Nutritionally derived glucose is actively concentrated in **brush border cells** of the intestinal epithelium by a Na^+-dependent symport (Fig. 18-25). It is transported from these cells to the circulatory system via a passive-mediated glucose uniport located on the capillary side of the cell and

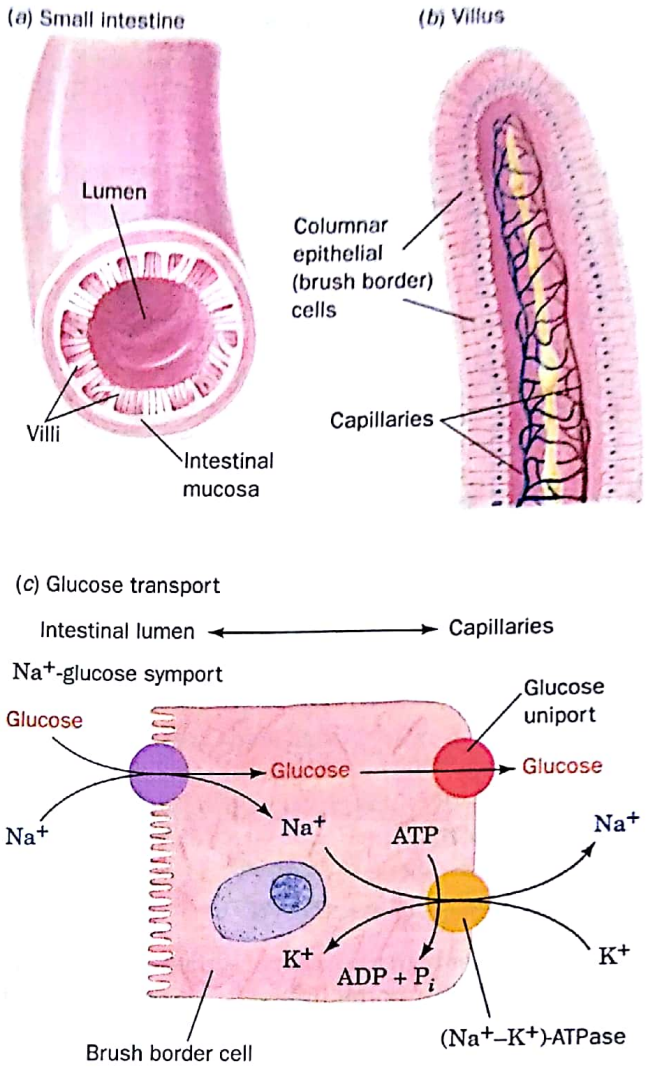


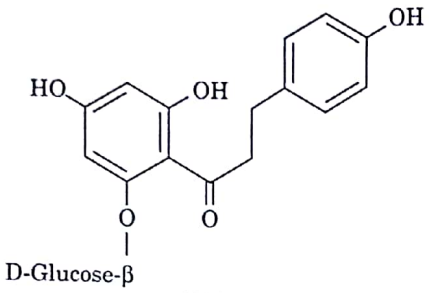
FIGURE 18-25. Glucose transport in the intestinal epithelium. The brushlike villi lining the small intestine greatly increase its surface area, thereby facilitating the absorption of nutrients. The brush border cells from which the villi are formed actively concentrate glucose from the intestinal lumen in symport with Na^+, a process that is driven by the $(Na^+–K^+)$–ATPase, which is located on the capillary side of the the cell and functions to maintain a low internal $[Na^+]$. The glucose is exported to the bloodstream via a separate passive-mediated uniport system like that in the erythrocyte.

which is similar to that of the erythrocyte membrane (Section 18-2B). Note that *although the immediate energy source for glucose transport from the intestine is the Na^+ gradient, it is really the free energy of ATP hydrolysis that powers this process through the maintenance of the Na^+ gradient by the $(Na^+–K^+)$–ATPase.* Nevertheless, since glucose enhances Na^+ resorption, which in turn enhances water resorption, glucose is often fed to individuals suffering from salt and water losses resulting from diarrhea.

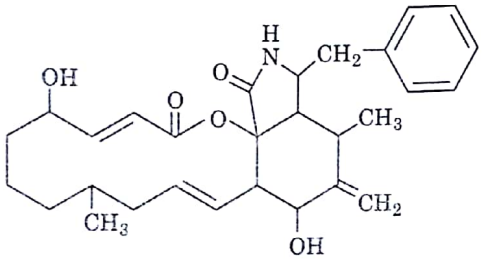
Active and Passive Glucose Transporters Exhibit Differential Drug Susceptibilities

The two glucose transport systems are inhibited by different drugs:

1. **Phlorizin** inhibits Na^+-dependent glucose transport.
2. **Cytochalasin B** inhibits Na^+-independent glucose transport.



Phlorizin



Cytochalasin B

Phlorizin binds only to the external surface of the Na^+-dependent glucose transporter, whereas cytochalasin B binds to the cytoplasmic surface of the Na^+-independent glucose transporter. This further indicates that these proteins are asymmetrically inserted into membranes. The use of these inhibitors permits the actions of the two glucose transporters to be studied separately in intact cells.

Kinetic studies indicate that the Na^+–glucose symport binds its substrates, Na^+ and glucose, in random order (Fig. 18-26) although binding of Na^+ increases the affinity of the transporter for glucose to such an extent that the upper pathway is heavily favored. Only when both substrates are bound, however, does the protein change its conformation to expose the binding sites to the inside of the cell. This requirement for concomitant Na^+ and glucose transport prevents the wasteful dissipation of the Na^+ gradient.

B. Lactose Permease

Gram-negative bacteria such as *E. coli* contain several active transport systems for concentrating sugars. We have already discussed the PTS system. Another extensively studied system, **lactose permease** (also known as **galactoside permease**), *utilizes the proton gradient across the bacterial cell membrane to cotransport H^+ and lactose (Fig. 18-27).* The proton gradient is metabolically generated through oxidative metabolism in a manner similar to that in mitochondria (Section 20-3B). The electrochemical potential gradient created by both these systems is used mainly to drive the synthesis of ATP.

How do we know that lactose transport requires the presence of a proton gradient? Ronald Kaback has established the requirement for this gradient through the following observations:

1. The rate of lactose transport into bacteria is increased enormously by the addition of D-lactate, an energy source for transmembrane proton gradient generation. Conversely, inhibitors of oxidative metabolism, such as cyanide, block both the formation of the proton gradient and lactose transport.
2. 2,4-Dinitrophenol, a proton ionophore that dissipates transmembrane proton gradients (Section 20-3D), inhibits lactose transport into both intact bacteria and membrane vesicles.

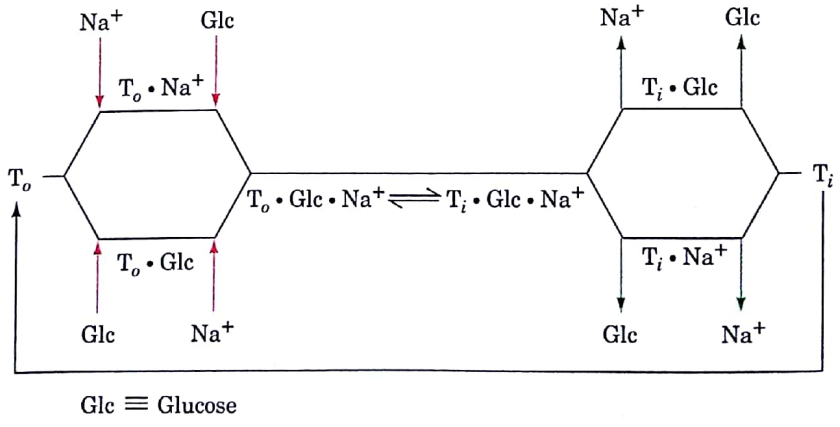


FIGURE 18-26. The Na^+-glucose symport system represented as a Random Bi Bi kinetic mechanism, although binding of Na^+ increases the affinity of the transporter for glucose to such an extent that the upper pathway is heavily favored. T_o and T_i, respectively, represent the transport protein with its binding sites exposed to the outer and inner surfaces of the membrane. [After Crane, R.K., and Dorando, F.C., *in* Martonosi, A.N. (Ed.), *Membranes and Transport,* Vol. 2, *p.* 154, Plenum Press (1982).]

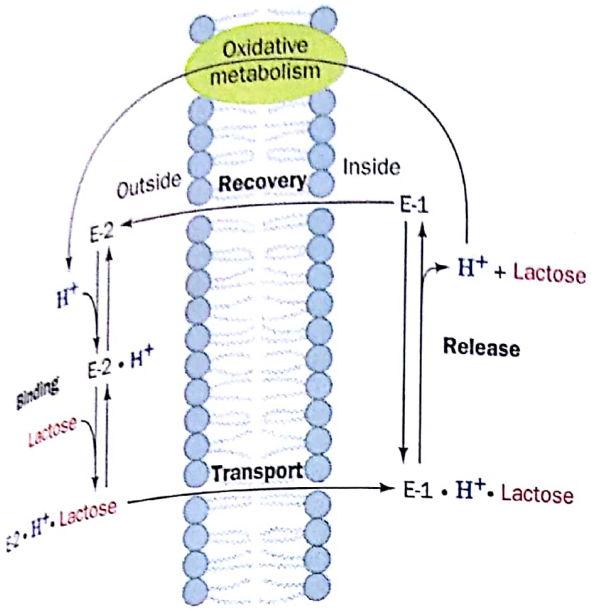
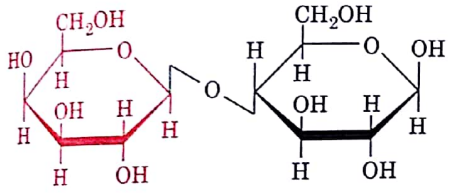
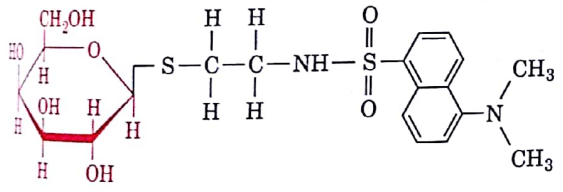


FIGURE 18-27. Kinetic mechanism of lactose permease in *E. coli*. H^+ binds first to E-2 outside the cell, followed by lactose. They are released in random order from E-1 inside the cell. E-2 must bind both lactose and H^+ in order to change conformation to E-1, thereby cotransporting these substances into the cell. E-1 changes conformation to E-2 when neither lactose nor H^+ is bound, thus completing the transport cycle.

3. The fluorescence of **dansylaminoethylthiogalactoside,**



Lactose



Dansylaminoethylthiogalactoside

a competitive inhibitor of lactose transport, is sensitive to the polarity of its environment and thus changes when it binds to lactose permease. Fluorescence measurements indicate that it does not bind to membrane vesicles that contain lactose permease in the absence of a transmembrane proton gradient.

Lactose Permease Has Two Major Conformational States

Lactose permease, like the (Na^+-K^+)-ATPase, is a transmembrane protein with two major conformational states (Fig. 18-27):

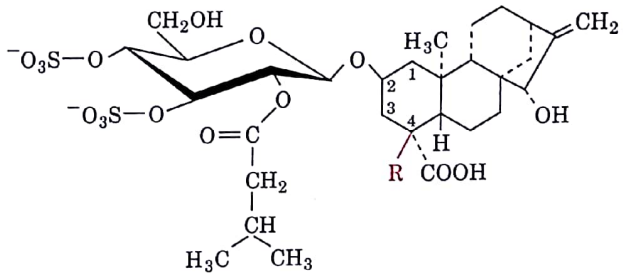
1. E-1, which has a low-affinity lactose-binding site facing the interior of the cell.
2. E-2, which has a high-affinity lactose-binding site facing the exterior of the cell.

E-1 and E-2 can only interconvert when their H^+ and lactose-binding sites are either both filled or both empty. This prevents both dissipation of the H^+ gradient without cotransport of lactose into the cell, and transport of lactose out of the cell without cotransport of H^+ against its concentration gradient.

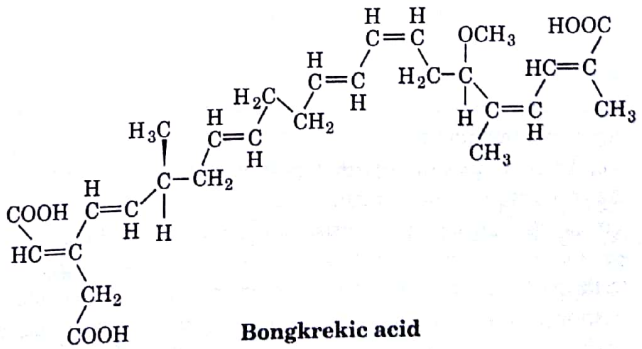
C. ADP-ATP Translocator

ATP generated in the mitochondrial matrix (its inner compartment; Section 1-2A) through oxidative phosphorylation (Section 20-3C) is largely utilized in the cytosol to drive such endergonic processes as biosynthesis, active transport, and muscle contraction. The inner mitochondrial membrane contains a system that transports ATP out of the matrix in exchange for ADP produced in the cytosol by ATP hydrolysis. This antiport, **ADP-ATP translocator,** is electrogenic since it exchanges ADP^{3-} for ATP^{4-}.

Several natural products inhibit ADP-ATP translocation. **Atractyloside** and its derivative **carboxyatractyloside** inhibit the process only from the external surface of the inner mitochondrial membrane; **bongkrekic acid** exerts its effects only on the internal surface.



R = H **Atractyloside**
R = COOH **Carboxyatractyloside**



Bongkrekic acid

These differentially acting inhibitors have been valuable tools in the isolation of the transport protein and in the elucidation of its mechanism of action. For example, the

translocator has been purified by affinity chromatography (Section 5-3D) using atractyloside derivatives as affinity ligands. Atractyloside binding is also a convenient means of identifying the translocator.

The ADP–ATP translocator, a dimer of identical 30-kD subunits, has characteristics similar to those of other transport proteins. It has one binding site for which ADP and ATP compete. It has two major conformations, one with its ATP–ADP binding site facing the inside of the mitochondrion, and the other with this site facing outward (Fig. 18-28). The translocator is an antiport because it must bind ligand to change from one conformational state to the other at a physiologically reasonable rate.

The ADP–ATP translocator is not itself an active transport system. However, its electrogenic export of one negative charge per transport cycle in the direction of ATP export–ADP import is driven by the membrane potential difference, $\Delta\Psi$, across the inner mitochondrial membrane (positive outside). This results in the formation of gradients in ATP and ADP across the membrane.

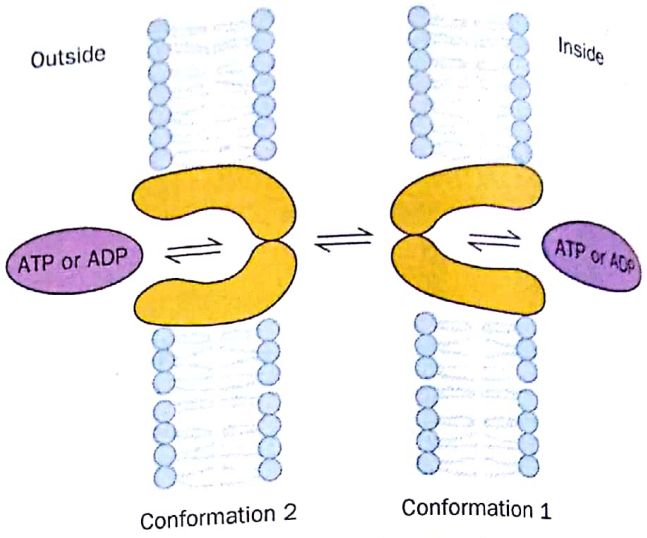


FIGURE 18-28. Conformational mechanism of the ADP–ATP translocator. An adenine nucleotide–binding site located in the intersubunit contact area of the translocator dimer is alternately exposed to the two sides of the membrane. In contrast to the glucose transporter (Fig. 18-15), the ADP–ATP translocator can change its conformation only when bound to ADP or ATP.

CHAPTER SUMMARY

Polar molecules and ions are transported across biological membranes by specific transmembrane transport proteins. The free energy change of the species transported depends on the ratio of its concentrations on the two sides of the membrane and, if the species is charged, on the membrane potential $\Delta\Psi$. The rate of nonmediated diffusion across a membrane is a linear function of the difference in concentration of the species on the two sides of the membrane as governed by Fick's first law of diffusion. Mediated transport is characterized by rapid saturation kinetics and specificity for the substance transported. It is also subject to competitive inhibition and chemical inactivation. Ionophores transport ions through membranes. Carrier ionophores, such as valinomycin, do so by wrapping a specific ion in a hydrophobic, membrane-soluble coat that can freely diffuse through the membrane. Channel-forming ionophores, such as gramicidin A, form a transmembrane pore through which selected ions can diffuse. The ion selectivity of porins varies with the identities of the amino acid side chains lining the transmembrane channel. Glucose transport across erythrocyte membranes is mediated by a dimeric transmembrane glycoprotein that can assume two conformations: one with a glucose-binding site facing the external cell surface and the other with the glucose site facing the cytosol. Transport occurs by the binding of glucose to the protein on one face of the membrane, followed by a conformational change that closes this site and exposes the other (a gated pore).

Active transport of molecules or ions against a concentration gradient requires an input of free energy. The free energy of ATP hydrolysis is coupled to the transport of three Na^+ ions out of and two K^+ ions into the cell by the $(Na^+–K^+)$–ATPase. This electrogenic process involves phosphorylation of an Asp residue (by ATP) in the presence of Na^+ and its dephosphorylation (hydrolysis) in the presence of K^+. Phosphorylation and dephosphorylation are accompanied by conformational changes that ensure rapid interconversion of all intermediates along the transport pathway. ATP-driven transport of Ca^{2+} by the Ca^{2+}·calmodulin-activated Ca^{2+}-ATPase and of H^+ by $(H^+–K^+)$–ATPase occur by similar phosphorylation/dephosphorylation mechanisms. Bacteria transport sugars by group translocation, a process in which the transported substance is chemically modified. The PTS system, which has important regulatory functions, phosphorylates sugars as they are transported by utilizing phosphoenolpyruvate as a phosphoryl donor.

Active transport may be driven by the free energy stored in ion gradients (secondary active transport). Glucose is transported into intestinal epithelial cells against its concentration gradient by a Na^+–glucose symport. This process is ultimately powered by the free energy of ATP hydrolysis since the Na^+ gradient is constantly being replenished via the $(Na^+–K^+)$–ATPase. The system conforms to a Random Bi Bi kinetic mechanism, implying that both Na^+ and glucose must be bound for the transport-producing conformational change to occur. Lactose is transported into *E. coli* by lactose permease, an H^+–lactose symport. This process is driven by the cell's electrochemical H^+ gradient which is, in turn, maintained by a proton pump coupled with oxidative metabolism. The mitochondrial ADP–ATP antiport system also interacts with the membrane potential in the asymmetric transport of ATP out of and ADP into the mitochondrion.